

<https://helda.helsinki.fi>

Lateglacial and Holocene climate change in the NE Tibetan Plateau : Reconciling divergent proxies of Asian summer monsoon variability

Li, Yuan

2021-04

Li, Y , Qiang , M , Huang , X , Zhao , Y , Leppänen , J , Weckström , J & Väliranta , M 2021 , ' Lateglacial and Holocene climate change in the NE Tibetan Plateau : Reconciling divergent proxies of Asian summer monsoon variability ' , CATENA , vol. 199 , 105089 . <https://doi.org/10.1016/j.catena.2020.105089>

<http://hdl.handle.net/10138/351971>

<https://doi.org/10.1016/j.catena.2020.105089>

cc_by_nc_nd

acceptedVersion

Downloaded from Helda, University of Helsinki institutional repository.

This is an electronic reprint of the original article.

This reprint may differ from the original in pagination and typographic detail.

Please cite the original version.

Catena

Lateglacial and Holocene climate change in the NE Tibetan Plateau: Reconciling divergent proxies of Asian summer monsoon variability

--Manuscript Draft--

Manuscript Number:	CATENA12929R1
Article Type:	Research Paper
Keywords:	Holocene; monsoon; China; Micropaleontology; lake level; vegetation.
Corresponding Author:	Mingrui Qiang Guangzhou, Guangdong CHINA
First Author:	Yuan Li
Order of Authors:	Yuan Li Mingrui Qiang Xiaozhong Huang Yongtao Zhao Jaakko Leppänen Jan Weckström Minna Väliranta
Abstract:	<p>The nature of Holocene Asian summer monsoon (ASM) evolution documented by diverse natural archives remains controversial, with a contentious issue being whether or not a strong Asian summer monsoon prevailed during the early Holocene. Here we present sequences of multiple proxies measured in sediment cores from Genggahai Lake in the NE Tibetan Plateau (NETP). The results suggest that a higher lake level and relatively lower terrestrial vegetation cover occurred synchronously during the early Holocene (11.3–8.6 kyr cal BP), compared with the period from 8.6 to 6.9 kyr cal BP. This finding clearly reflects the existence of different hydroclimatic conditions between the lake and its catchment due to diverse driving mechanisms. The early Holocene high stand of the lake, as demonstrated by the stratigraphic variability of the remains of aquatic biota, may have responded to the strengthened ASM and increased monsoonal precipitation; the relatively low vegetation cover in the marginal region of the Asian monsoon during the early Holocene, and the coeval widespread active sand dune mobility in both the NE Tibetan Plateau and NE China, most likely resulted from a low level of effective moisture due to high evaporation, and hence they cannot be interpreted as evidence of a weak ASM. Our results potentially reconcile the current divergent interpretations of various proxy climate records from the region. Our findings suggest that the ASM evolution was characterized by a consistent pattern across the monsoonal regions, as indicated by the oxygen isotope record of Chinese speleothems.</p>

Catena
Editor

November 26, 2020

Dear Editor,

We are resubmitting a manuscript, entitled 'Lateglacial and Holocene climate change in the NE Tibetan Plateau: Reconciling divergent proxies of Asian summer monsoon variability' with a reference code of CATENA12849. We thank you for your efforts to evaluate this work.

In light of the comments and suggestions raised by the reviewers, we have carefully revised the manuscript. The major revisions are outlined as follows:

We made small adjustments to the zonation of biota stratigraphy according to reviewer #1's comments, highlighting that a higher lake level and relatively lower terrestrial vegetation cover occurred synchronously during the early Holocene (11.3–8.6 kyr cal BP), compared with the period from 8.6 to 6.9 kyr cal BP.

We hope that the revisions are satisfactory to you. Please let us know if you have any questions regarding the revisions. Thank you!

Yours sincerely,

Yuan Li and other co-authors

- Early Holocene high lake level and low vegetation cover occurred synchronously.
- Early Holocene high lake level suggests stronger monsoonal circulation.
- Early Holocene low vegetation cover did not reflect a weakened monsoon.

1 **Lateglacial and Holocene climate change in the NE Tibetan Plateau: Reconciling**
2 **divergent proxies of Asian summer monsoon variability**

3 **Yuan Li^{a, c}, Mingrui Qiang^{b, c*}, Xiaozhong Huang^c, Yongtao Zhao^a, Jaakko J. Leppänen^d,**
4 **Jan Weckström^d, Minna Väliranta^d**

5 ^a Key Laboratory of Desert and Desertification, Northwest Institute of Eco-Environment and
6 Resources, Chinese Academy of Sciences, Lanzhou 730000, China.

7 ^b School of Geography, South China Normal University, Guangzhou 510631, China

8 ^c Key Laboratory of Western China's Environmental Systems (MOE), College of Earth and
9 Environmental Sciences, Lanzhou University, Lanzhou 730000, China.

10 ^d Environmental Change Research Unit, Ecosystems and Environment Research Programme and
11 Helsinki Institute of Sustainability Science, Faculty of Biological and Environmental Sciences,
12 P.O. Box 65, 00014 University of Helsinki, Finland.

13 Corresponding author: Mingrui Qiang (mrqiang@scnu.edu.cn).

14 **Abstract**

15 The nature of Holocene Asian summer monsoon (ASM) evolution documented by diverse
16 natural archives remains controversial, with a contentious issue being whether or not a strong
17 Asian summer monsoon prevailed during the early Holocene. Here we present sequences of
18 multiple proxies measured in sediment cores from Genggahai Lake in the NE Tibetan Plateau
19 (NETP). The results suggest that a higher lake level and relatively lower terrestrial vegetation
20 cover occurred synchronously during the early Holocene (11.3–8.6 kyr cal BP), compared with
21 the period from 8.6 to 6.9 kyr cal BP. This finding clearly reflects the existence of different
22 hydroclimatic conditions between the lake and its catchment due to diverse driving mechanisms.
23 The early Holocene high stand of the lake, as demonstrated by the stratigraphic variability of the
24 remains of aquatic biota, may have responded to the strengthened ASM and increased monsoonal
25 precipitation; the relatively low vegetation cover in the marginal region of the Asian monsoon
26 during the early Holocene, and the coeval widespread active sand dune mobility in both the NE
27 Tibetan Plateau and NE China, most likely resulted from a low level of effective moisture due to
28 high evaporation, and hence they cannot be interpreted as evidence of a weak ASM. Our results
29 potentially reconcile the current divergent interpretations of various proxy climate records from
30 the region. Our findings suggest that the ASM evolution was characterized by a consistent
31 pattern across the monsoonal regions, as indicated by the oxygen isotope record of Chinese
32 speleothems.

33 *Key words:* Holocene; monsoon; China; Micropaleontology; lake level; vegetation.

34 **1 Introduction**

35 The Asian monsoon system affects more than half of the world's population and the
36 associated ecosystems (Webster et al., 1998). Understanding the variability of the Asian
37 monsoon has significant implications for the social and ecological systems in the region (Hansen
38 and Lebedeff, 1987; Mishra et al., 2019). Precipitation in the marginal regions dominated by the
39 Asian summer monsoon (ASM) is highly dependent on the strength of the ASM: a stronger ASM
40 circulation can transport more water vapor, leading to higher precipitation, and vice versa (Zhou
41 et al., 2009). Therefore, precipitation in these marginal regions can directly reflect the strength of
42 the ASM (Chen et al., 2015). Over the past two decades, numerous studies of the Holocene
43 evolution of the ASM have been conducted based on diverse natural archives from the region
44 (e.g., Chen et al., 2015; Dykoski et al., 2005; Goldsmith et al., 2017; Hu et al., 2008; Li et al.,
45 2014; Wang et al., 2005; Wei et al., 2020). However, the nature of ASM evolution during the
46 Holocene still remains controversial, with a contentious issue being whether or not a strong
47 Asian summer monsoon prevailed during the early Holocene. For example, the early Holocene
48 high-stand of lakes in the marginal regions dominated by the ASM (Fig. 1A), including lakes
49 Dali (Goldsmith et al., 2017), Dabusu (Li and Lv, 2001) and Kuhai (Mischke et al., 2010),
50 reflects an intensified ASM which is consistent with monsoonal records from Chinese
51 speleothems (Dykoski et al., 2005; Hu et al., 2008; Wang et al., 2005). However, records of
52 pollen assemblages and/or pollen-based precipitation from the lakes in the region (Fig. 1A),
53 including lakes Gonghai (Chen et al., 2015), Dalianhai (Cheng et al., 2013), Daihai (Xiao et al.,
54 2004), Dali (Wen et al., 2017) and Hulun (Wen et al., 2010), together with evidence for
55 widespread sand dune mobility in NE China (Li et al., 2014), indicate the occurrence of dry
56 terrestrial conditions at this time, possibly related to a weak ASM. Furthermore, even diverse
57 proxies generated from the same study site may exhibit divergent patterns of Holocene climate
58 change and ASM evolution. For example, at Qinghai Lake, the geochemical proxies (An et al.,
59 2012; Jin et al., 2015; Lister et al., 1991) generally suggest a high lake level and a strong ASM
60 during the early Holocene. In contrast, the shoreline deposits (Liu et al., 2015) and the pollen
61 assemblages (Shen et al., 2005) suggest that the lake level probably was low at this time, induced
62 by high evaporation or a weak ASM. These seemingly contradictory interpretations, especially
63 those from the same site (e.g., Qinghai Lake), cannot be explained by the spatial and temporal
64 differentiation of ASM evolution, or by chronological uncertainties. Therefore, a comprehensive
65 analysis of the driving mechanisms of these proxies and their linkage to the ASM are essential
66 for reconciling the controversy.

67 Genggahai Lake is a small, shallow lake in the NE Tibetan Plateau (NETP) (Fig. 1A),
68 located in the marginal region dominated by the ASM. The sediments are rich in the remains of
69 aquatic biota and terrestrial pollen, which provide the opportunity to conduct multi-proxy
70 investigations of ASM evolution. Qiang et al. (2013b) have discussed the lake-level fluctuations
71 over the past 16 kyr based mainly on plant macrofossil assemblages in the sediments from a
72 single core (GGH-A) recovered from the lake. However, the early Holocene high-stand of the
73 lake was indirectly inferred by geochemical variables (total organic carbon, total nitrogen and
74 carbon isotopic composition of bulk sediment organic matter), due to the absence of plant
75 macrofossils (Qiang et al., 2013b). In addition, the evolution of lake bathymetry may also lead to
76 lake-level fluctuations on a long timescale (Hilton, 1985; Lehman, 1975), which was not
77 differentiated from the influence of climatic factors in the previous study (Qiang et al., 2013b).
78 Therefore, comprehensive analyses of diverse bioindicators (e.g., plant macrofossils, Cladocera,
79 diatoms) from multiple cores are essential not only for the reliable reconstruction of lake-level
80 fluctuations, but also for assessing the influence of the evolution of lake bathymetry on the lake-
81 level fluctuations, and for understanding regional hydroclimatic changes (Dearing, 1997).
82 Moreover, the evolution of the regional terrestrial vegetation and its potential linkages to the
83 ASM remain unclear.

84 Here we present sequences of aquatic (plant macrofossils, Cladocera, diatoms) and
85 terrestrial (terrestrial pollen) proxies derived from multiple sediment cores from Genggahai
86 Lake. Combined with hydrological and ecological investigations of the modern lake, and with
87 reference to independent climatic records from the marginal regions dominated by the ASM, our
88 aims were to reconstruct the regional ASM variability during the Lateglacial and the Holocene,
89 and to reconcile the current divergent results of proxy indicators of ASM evolution.

90 **2 Materials and Methods**

91 Genggahai Lake (36°11'N, 100°06'E) is located in the central Gonghe Basin (Fig. 1B) at
92 an altitude of 2,860 m a.s.l. The lake is small (surface area, ~2 km²) and shallow (maximum
93 water depth, ~1.8 m) and has an elevated salinity (~1.2 g L⁻¹) and pH (~9.1). *Potamogeton*
94 *pectinatus*, *Myriophyllum spicatum*, and *Chara* spp. dominate the submerged macrophyte
95 communities in the current lake. The lake is mainly fed by groundwater. Several small spring-
96 water streams flow into the lake. Three sediment cores were recovered from Genggahai Lake in
97 January 2008 and January 2013 using a modified Livingstone piston corer. Cores GGH-A (length
98 782 cm) and GGH-C (length 774 cm) were recovered from the center of the lake in a water depth
99 of 170 cm (Fig. 1C), and core GGH-E (length 765 cm) was recovered from the northwest littoral
100 area in a water depth of 110 cm (Fig. 1C). Due to the lack of terrestrial plant remains, samples of

101 the leaves of aquatic macrophytes were picked from the sediments for accelerator mass
102 spectrometry (AMS) ^{14}C dating, conducted by Beta Analytic Inc. (Miami, USA) (Table S1). The
103 reservoir age of the lake was estimated at 1,010 ^{14}C years on average, based on the AMS ^{14}C
104 dating results of the dissolved inorganic carbon of the lake water, macrophyte remains in the
105 lake's surface sediments and living *P. pectinatus* (Li et al., 2017b). A total of 26 ^{14}C ages from
106 cores GGH-A (cited from Qiang et al. 2013b), GGH-C, and GGH-E (Table S1), which are in
107 stratigraphic order, were calibrated to calendar years (Calib 6.0.1, Reimer et al., 2009) after
108 subtracting an average reservoir age (1,010 yr). The age-depth models of the three cores were
109 generated by the Bacon Bayesian age-modeling software (Blaauw and Christen, 2011), using the
110 calibrated radiocarbon ages. The age versus depth profiles of the three cores agree well with each
111 other, which supports their reliability (Fig. S1).

112 Plant macrofossils, including *Chara* gyrogonites (Fig. 2B, 2D, 2F) and encrustations of
113 *Chara* spp. and *P. pectinatus* (or *M. spicatum*) (Fig. 2A, 2C, 2E), were picked from cores GGH-
114 A (cited from Qiang et al. 2013b), GGH-C, and GGH-E. Cladocera (Fig. 2G) and diatom (Fig. 2I,
115 2G) analyses were conducted on core GGH-C using standard methods (Korhola and Rautio,
116 2001; Weckström et al., 1997). In addition, fossil pollen (Fig. 3A, 3C) was extracted from core
117 GGH-A following the methods of Fægri and Iversen (1989). In order to comprehensively depict
118 the terrestrial vegetation conditions in the marginal regions dominated by the ASM, we compiled
119 six lacustrine tree pollen records from the region, including from lakes Qinghai (Shen et al.,
120 2005), Dalianhai (Cheng et al., 2013), Gonghai (Chen et al., 2015), Dali (Wen et al., 2017),
121 Daihai (Xiao et al., 2004) and Hulun (Wen et al., 2010). Since the changes in the tree pollen
122 content of these records show a similar trend, a synthesized tree pollen index covering the past
123 12 kyr (obtained by taking the average of the normalized tree pollen contents from the six lakes)
124 was used to portray changes in tree cover in the marginal regions dominated by the ASM
125 (Fig. 3). Further details about the method are given in the supplements.

126 **3 Results and discussion**

127 3.1. Patterns of hydroclimatic evolution indicated by lake level and pollen sequences

128 In general, submerged macrophytes, Cladocera, and diatoms in freshwater lakes are
129 sensitive to changes in water level, and thus their fossil remains in lake sediments can be used to
130 reconstruct past water-level fluctuations (Birks, 1993; Heggen et al., 2012). The aquatic plant
131 macrofossils in the sediments of Genggahai Lake mainly originate from *Chara* spp.,
132 *P. pectinatus* and *M. spicatum*. These species also dominate the lake today and they are common
133 in shallow lakes worldwide (Wilson et al., 1941). The spatial distribution of submerged
134 macrophytes in the modern lake is mainly modulated by the water depth, and the shallow water

135 zone of the lake is occupied by *Chara* spp. (Fig. S2) (Qiang et al., 2013b). Therefore, the
136 occurrence of the fossil remains of *Chara* spp. and *P. pectinatus* (or *M. spicatum*) in the lake
137 sediments, especially the occurrence of abundant *Chara* gyrogonites, most likely reflects a
138 shallow water environment. As for fossil Cladocera, only two littoral species (*Chydorus*
139 *sphaericus* and *Coronatella rectangula*) which prefer macrophyte habitats were identified in the
140 sediments of Lake Genggahai (Walseng, B., 2016a, 2016b). Diatoms in the sediments are
141 relatively diverse, consisting of both planktonic (e.g., *Lindavia comta* and *Cyclotella*
142 *distinguenda*) and non-planktonic species (e.g., *Gomphonema angustum* and *Achnanthes*
143 *minutissima*). Based on changes in submerged macrophytes, Cladocera and diatoms in the lake
144 sediments (Fig. 2), the history of lake-level fluctuations was divided into the following four
145 stages:

146 **15.4–11.3 cal kyr BP** The lake sediments contain abundant submerged-macrophyte
147 encrustations, *Chara* gyrogonites and littoral cladoceran fossils, reflecting a shallow lake. In
148 addition, the diatom assemblages are dominated by both planktonic (e.g., *L. comta* and *C.*
149 *distinguenda*) and non-planktonic species (e.g., *G. angustum*). Notably, *C. distinguenda* is a
150 *tychoplanktonic species* which can adapt to shallow water conditions. Therefore, the lake level
151 most likely was low during this period.

152 **11.3–8.6 cal kyr BP** Submerged macrophytes and Cladocera largely disappear from the
153 sediments. In addition, the diatom assemblages are dominated by an euplanktonic species (i.e., *L.*
154 *comta*). Thus we conclude that the lake level was high during this period, and it may have
155 exceeded the depth limit for submerged macrophytes, resulting in the absence of Cladocera
156 macrophyte habitats and increasing the abundance of planktonic diatoms.

157 **8.6–5.5 cal kyr BP** Submerged macrophyte encrustations occur episodically and *Chara*
158 gyrogonites are relatively scarce. Cladocera fossils largely disappear from the sediments,
159 probably in response to the scarcity of macrophyte habitats. The diatom assemblages are
160 dominated by both planktonic (e.g., *L. comta* and *C. distinguenda*) and non-planktonic species.
161 Thus we conclude that the lake level during this period was probably high overall, but lower than
162 during the previous stage.

163 **5.5 kyr cal BP to the present** The lake sediments contain abundant submerged-
164 macrophyte encrustations, *Chara* gyrogonites, littoral Cladocera fossils, and non-planktonic
165 diatoms, reflecting a shallow lake.

166 The terrestrial pollen in lake sediments is mainly derived from the catchment and hence it
167 reflects the local and regional terrestrial vegetation conditions (Pennington, 1979). Changes in
168 total terrestrial pollen concentrations (Fig. 3A) and tree pollen contents (Fig. 3C) in the

169 sediments of Genggahai Lake are largely in agreement with those at nearby Qinghai Lake (Fig.
170 3B, 3D) and the synthesized tree pollen index (Fig. 3J), showing that optimal vegetation
171 conditions occurred during 8.6–6.9 cal kyr BP. Overall, the aquatic and animal fossils
172 (macrophytes, Cladocera, diatoms) and terrestrial pollen in the sediments of Genggahai Lake
173 indicate that a higher lake level and relatively lower terrestrial vegetation cover occurred
174 synchronously during the early Holocene (11.3–8.6 kyr cal BP), compared with the period from
175 8.6 to 6.9 kyr cal BP. This implies the occurrence of different hydroclimatic conditions between
176 the lake and its catchment (Fig. 4A, 4I). This apparent contradiction is also reflected in proxy
177 sequences from other lakes in the marginal regions dominated by the ASM: e.g., at Lakes
178 Qinghai (An et al., 2012; Shen et al., 2005), Dali (Goldsmith et al., 2017; Wen et al., 2017) and
179 Chagan Nur (Li et al., 2020a).

180 3.2. Implications for the evolution of the Asian summer monsoon

181 The early Holocene high lake levels and low total pollen concentrations (or tree
182 percentages) recorded by lake sediments from the margins of the regions dominated by the ASM
183 are mutually contradictory in terms of their interpretation as evidence for ASM strength (e.g., An
184 et al., 2012; Chen et al., 2015), or as evidence for the spatial differentiation of ASM evolution
185 (Zhang et al., 2019). However, these seemingly contradictory patterns most likely reflect the
186 existence of different hydroclimatic conditions between the lake and its catchment due to diverse
187 driving mechanisms (cf., Wilson et al., 2015), and they cannot simultaneously be interpreted as
188 proxies of ASM strength.

189 In general, lake-level fluctuations are controlled by the water balance of the lake.
190 However, previous studies have demonstrated that the evolution of lake bathymetry on a long
191 timescale may also result in lake-level fluctuations (Hilton, 1985; Lehman, 1975). Increased
192 allochthonous input of detrital materials will enhance the sedimentation rate in the deepest parts
193 of the lake due to gravity (i.e., the “sediment-focusing effect”) which will lead to decreases in
194 water depth (Hilton, 1985). However, at Genggahai Lake, the AMS ¹⁴C dating results show that
195 the sedimentation rate of the central cores (GGH-A and GGH-C) was largely consistent with that
196 of the littoral core (GGH-E) during the Lateglacial and Holocene (Fig. S1), indicating that
197 changes in lake bathymetry since the Lateglacial were probably minor, exerting little effect on
198 the lake level. This could be ascribed to the flat lake basin morphometry and the dense growth of
199 submerged macrophytes, which largely restricted re-suspension and transport of sediments to the
200 depocenter (cf. Dearing, 1997). Therefore, lake-level fluctuations mainly represent the balance
201 between water inflows and losses. Currently, there are no large glaciers on the summits of the
202 mountains surrounding Genggahai Lake. In addition, the Lateglacial glaciers on these mountains

203 were mainly distributed in areas above 4,500 m a.s.l. (Fig. 1B) (Li et al., 1991) and therefore
204 their total extent was relatively small. Thus they are unlikely to have continuously contributed
205 meltwater which could sustain the high lake level during the early Holocene (11.3–8.6 kyr
206 BP), given the temperature increase of ~3 °C at the onset of the Holocene (Herzschuh et al., 2014;
207 Li et al., 2017a). Genggahai Lake is fed mainly by groundwater. Loose, porous fluvio-lacustrine
208 sediments of the Gonghe Formation (Perrineau et al., 2011) and surficial fluvial-fan sediments
209 largely constitute the catchment substrate of groundwater. In addition, the deep incision of the
210 Yellow River in the eastern Gonghe Basin led to a steep hydraulic gradient of the basin
211 (Craddock et al., 2010). Therefore, the catchment of groundwater was highly permeable, and
212 hence precipitation can infiltrate rapidly into the ground and feed the lake. The evaporation
213 losses during the infiltration process were most likely low. In addition, the catchment area of the
214 groundwater feeding the lake is far larger than the lake's surface area (Fig. 1B). Therefore,
215 evaporation may play a minor role in the water balance of the lake, and hence the lake-level
216 fluctuations can be interpreted as indicating changes in regional precipitation, reflecting the
217 strength of the ASM in the study area. The pattern of water-level fluctuations at Genggahai Lake
218 largely coincides with that of other lakes in the marginal regions dominated by the ASM (e.g.,
219 Qinghai, Kuhai, Dali, Dabusu and Chagan Nur) (Fig. 4B–F). This consistent pattern suggests a
220 weak ASM during 15.4–11.3 cal kyr BP, a significantly intensified ASM during 11.3–8.6 cal
221 kyr BP, and a gradually weakening ASM thereafter. In addition, the results of a modeling study
222 of water level changes at Qinghai Lake also reveal an early Holocene high-stand (Fig. 4C) (Li et
223 al., 2020b).

224 The evolution of terrestrial vegetation is generally the integrated reactions to multiple
225 environmental factors, including temperature, precipitation and the available water capacity of
226 the soil (Prentice et al., 1992). The sparse terrestrial vegetation in the marginal regions
227 dominated by the ASM during 15.4–11.3 cal kyr BP and 5.5–0 cal kyr BP mainly resulted from
228 low monsoonal precipitation and low temperatures (Lu et al., 2011). In addition, the relatively
229 low total terrestrial pollen concentration (Fig. 4I) during the early Holocene (11.3–8.6 kyr cal BP)
230 suggests that the terrestrial vegetation did not respond to the significantly ameliorated
231 environmental conditions, although the monsoonal precipitation increased sharply. Significantly,
232 changes in terrestrial vegetation are modulated mainly by effective moisture rather than by
233 precipitation (Prentice et al., 1992). Furthermore, changes in effective moisture do not always
234 respond linearly to variations in precipitation, but rather they depend on the balance between
235 precipitation and evaporation. Therefore, the relatively low terrestrial vegetation cover in the
236 study area during the early Holocene mostly likely reflects a low level of effective moisture.
237 Notably, the low effective moisture during this interval is also documented by the widespread

238 sand dune mobility in both the NETP and NE China (Fig. 4K, 4L) (Li et al., 2014; Qiang et al.,
239 2013a). Given that the enhanced monsoonal precipitation during the early Holocene may have
240 infiltrated rapidly into the ground due to the porous nature of the soils and the steep hydraulic
241 gradient of the catchment, the water retained in the soils probably could not compensate for the
242 intense evaporation loss as a consequence of the high temperatures (Li et al., 2017a) and high
243 summer insolation. This may have led to a low level of effective moisture and further restricted
244 the development of both the terrestrial vegetation and paleosols (Mason et al., 2009; Qiang et al.,
245 2013a, 2016). In addition, the strong ASM during this period would have resulted in the strong
246 release of latent heat by water (Herzschuh et al., 2014), which may have further increased
247 temperatures and evaporation. By contrast, decreased temperatures (Li et al., 2017a), due to the
248 reduction in both summer insolation and release of latent heat by water vapor during the period
249 from 8.6 to 6.9 cal kyr BP, likely resulted in the weakened evaporation of soil water and hence
250 led to the widespread development of vegetation (Fig. 3) and palaeosols (Li et al., 2014; Qiang et
251 al., 2013a) in the marginal regions dominated by the ASM. In addition, given that the terrestrial
252 vegetation has a lagged response to precipitation changes, the different response rates of the lake
253 water and terrestrial vegetation to climate change may also have contributed to the occurrence of
254 different hydroclimatic conditions between Genggahai Lake and its catchment (Zhao et al.,
255 2017).

256 The diverse proxies derived from sediments of Genggahai Lake clearly reveal the
257 synchronous occurrence of high lake levels and relatively low terrestrial vegetation cover, which
258 are correlative with evidence for widespread sand dune mobility in the marginal regions
259 dominated by the ASM during the early Holocene. These features do not reflect different
260 climatic patterns, but rather they reflect different aspects of monsoonal climate change. The
261 consistent high-stand of the lakes from these monsoon margin areas suggests increased
262 monsoonal precipitation during the early Holocene, providing compelling evidences for the
263 spatial consistency of ASM evolution documented by oxygen isotopic records from Chinese cave
264 deposits (Cheng et al., 2019; Dykoski et al., 2005; Hu et al., 2008; Wang et al., 2005). The strong
265 ASM and the increased monsoonal precipitation in the marginal regions dominated by the ASM
266 during the early Holocene are ascribed to the enhanced thermal contrast between land and sea in
267 spring and summer due to the increased orbitally-induced summer insolation (Fig. 4G, 4H). The
268 relatively low terrestrial vegetation cover during the early Holocene, as well as the widespread
269 dune sands in eolian sections in both the NETP and NE China, most likely reflect low effective
270 moisture conditions due to high evaporation, and hence they cannot be interpreted as evidence of
271 a weak monsoon.

272 **4 Conclusions**

273 The water-level fluctuations of Genggahai Lake and the vegetation conditions in its
274 catchment were reconstructed from the aquatic biota and pollen preserved in the lake sediments.
275 The results suggest a higher lake level and a stronger ASM during 11.3–5.5 cal kyr BP,
276 compared to the intervals of 15.4–11.3 cal kyr BP and 5.5–0 cal kyr BP. However, the total
277 terrestrial pollen concentration indicates relatively lower terrestrial vegetation cover during the
278 early Holocene (11.3–8.6 cal kyr BP), compared with the period from 8.6 to 6.9 kyr cal BP. In
279 contrast to the lake-level fluctuations, the vegetation cover in the catchment cannot be used as a
280 proxy for variations in monsoonal precipitation and thus ASM strength. Rather, the relatively
281 low vegetation cover mainly reflects a low level of effective moisture conditions, as a result of
282 intense evaporation due to high temperatures during the early Holocene.

283 **Declaration of Competing Interest**

284 The authors declare that they have no known competing financial interests or personal
285 relationships that could have appeared to influence the work reported in this paper.

286 **Acknowledgments**

287 We thank Dr. J. Bloemendal for his helpful comments and language improvements. This
288 research was supported by the National Natural Science Foundation of China (grants 41901103,
289 41671190, 41271219 and 41807440), the National Key R&D Program of China (grant
290 2017YFA0603402), and the Foundation for Excellent Youth Scholars of the “Northwest Institute
291 of Eco-Environment and Resources”, CAS.

292 **References**

- 293 An, Z.S., Colman, S.M., Zhou, W.J., Li, X.Q., Brown, E.T., Timothy Jull, A.J., Cai, Y.J., Huang, Y.S., Lu,
294 X.F., Chang, H., Song, Y.G., Sun, Y.B., Xu, H., Liu, W.G., Jin, Z.D., Liu, X.D., Cheng, P., Liu, Y., Ai, L.,
295 Li, X.Z., Liu, X.J., Yan, L.B., Shi, Z.G., Wang, X.L., Wu, F., Qiang, X.K., Dong, J.B., Lu, F.Y., Xu,
296 X.W., 2012. Interplay between the Westerlies and Asian monsoon recorded in Lake Qinghai sediments
297 since 32 ka. *Sci. Rep.* 2, 619–625.
- 298 Berger, A., Loutre, M.F., 1991. Isolation values for the climate of the last 10 million years. *Quat. Sci. Rev.* 10,
299 297–317.
- 300 Birks, H.H., 1993. The importance of plant macrofossils in late glacial climatic reconstructions: an example
301 from western Norway. *Quat. Sci. Rev.* 12, 719–726.
- 302 Blaauw, M., Christen, J.A., 2011. Flexible paleoclimate age depth models using an autoregressive gamma
303 process. *Bayesian Anal.* 6, 457–474.

304 Chen, F.H., Xu, Q.H., Chen, J.H., Birks, H.J., Liu, J.B., Zhang, S.R., Jin, L., An, C.B., Telford, R.J., Cao, X.Y.,
305 Wang, Z.L., Zhang, X.J., Selvaraj, K., Lu, H.Y., Li, Y.C., Zheng, Z., Wang, H.P., Zhou, A.F., Dong, G.H.,
306 Zhang, J.W., Huang, X.Z., Bloemendal, J., Rao, Z.G., 2015. East Asian summer monsoon precipitation
307 variability since the last deglaciation. *Sci. Rep.* 5, 11186.

308 Cheng, B., Chen, F.H., Zhang, J.W., 2013. Palaeovegetational and palaeoenvironmental changes since the last
309 deglacial in Gonghe Basin, northeast Tibetan Plateau. *J. Geogr. Sci.* 23, 136–146.

310 Cheng, H., Zhang, H.W., Zhao, J.Y., Li, H.Y., Ning, Y.F., Kathayat, G., 2019. Chinese stalagmite
311 paleoclimate researches: A review and perspective. *Sci. China-Earth Sci.* 62, 1489–1513.

312 Craddock, W.H., Kirby, E., Harkins, N.W., Zhang, H.P., Shi, X.H., Liu, J.H., 2010. Rapid fluvial incision
313 along the Yellow River during headwater basin integration. *Nat. Geosci.* 3, 209–213.

314 Dearing, J.A., 1997. Sedimentary indicators of lake-level changes in the humid temperate zone: a critical
315 review. *J. Paleolimn.* 18, 1–14.

316 Dykoski, C.A., Edwards, R.L., Cheng, H., Yuan, D.X., Cai, Y.J., Zhang, M.L., Lin, Y.S., Qing, J.M., An, Z.S.,
317 Revenaugh, J., 2005. A high-resolution, absolute-dated Holocene and deglacial Asian monsoon record
318 from Dongge Cave, China. *Earth Planet. Sci. Lett.* 233, 71–86.

319 Fægri, K., Iversen, J., 1989. *Textbook of Pollen Analysis*, fourth ed. John Wiley & Sons, Chichester.

320 Gao, Y.X., Xu, S.Y., Guo, Q.Y., Zhang, M.L., 1962. Monsoon regions in China and regional climates. In: Gao,
321 Y.X. (Ed.), *Some Problems on East-Asia Monsoon*. Science Press, Beijing, pp. 49–63 (in Chinese).

322 Goldsmith, Y., Broecker, W.S., Xu, H., Polissar, P.J., deMenocal, P.B., Porat, N., Lan, J.H., Cheng, P., Zhou,
323 W.J., An, Z.S., 2017. Northward extent of East Asian monsoon covaries with intensity on orbital and
324 millennial timescales. *Proc. Natl. Acad. Sci.* 114, 1817–1821.

325 Hansen, J., Lebedeff, S., 1987. Global trends of measured surface air temperature. *J. Geophys. Res.-Atmos.* 92,
326 13345–13372.

327 Heggen, M.P., Birks, H.H., Heiri, O., Grytnes, J.A., Birks, H.J.B., 2012. Are fossil assemblages in a single
328 sediment core from a small lake representative of total deposition of mite, chironomid, and plant
329 macrofossil remains? *J. Paleolimn.* 48, 669–691.

330 Herzsuh, U., Borkowski, J., Schewe, J., Mischke, S., Tian, F., 2014. Moisture advection feedback supports
331 strong early-to-mid Holocene monsoon climate on the eastern Tibetan Plateau as inferred from a pollen-
332 based reconstruction. *Paleogeogr. Paleoclimatol. Paleoecol.* 402, 44–54.

333 Hilton, J.A., 1985. Conceptual framework for predicting the occurrence of sediment focusing and sediment
334 redistribution in small Lakes. *Limnol. Oceanogr.* 30, 1131–1143.

335 Hu, C.Y., Henderson, G.M., Huang, J.H., Xie, S.C., Sun, Y., Johnson, K.R., 2008. Quantification of Holocene
336 Asian monsoon rainfall from spatially separated cave records. *Earth Planet. Sci. Lett.* 266, 221–232.

337 Jin, Z.D., An, Z.S., Yu, J.M., Li, F.C., Zhang, F., 2015. Lake Qinghai sediment geochemistry linked to
338 hydroclimate variability since the last glacial. *Quat. Sci. Rev.* 122, 63–73.

- 339 Korhola, A., Rautio, M., 2001. Cladocera and other Branchiopod crustaceans. In: Smol, J.P., Birks, J.B., Last,
340 W.M. (Eds.), Tracking environmental change using lake sediments. Zoological indicators. Kluwer,
341 Dordrecht. pp. 5–41.
- 342 Lehman, J.T., 1975. Reconstructing the rate of accumulation of lake sediment: The effect of sediment focusing.
343 *Quat. Res.* 5, 541–550.
- 344 Li, G.Q., Wang, Z., Zhao, W.W., Jin, M., Wang, X.Y., Tao, S.X., Chen, C.Z., Cao, X.Y., Zhang, Y.N., Yang,
345 H., Madsen, D., 2020a. Quantitative precipitation reconstructions from Chagan Nur revealed lag response
346 of East Asian summer monsoon precipitation to summer insolation during the Holocene in arid northern
347 China. *Quat. Sci. Rev.* 239, 106365.
- 348 Li, J.J., Zhou, S.Z., Pan, B.T., 1991. The problems of Quaternary glaciation in the eastern part of Qinghai-
349 Xizang Plateau. *Quaternary Sciences* 3, 193–203 (in Chinese with English abstract).
- 350 Li, Q., Wu, H.B., Yu, Y.Y., Sun, A.Z., Markovic, S.B., Guo, Z.T., 2014. Reconstructed moisture evolution of
351 the deserts in northern China since the Last Glacial Maximum and its implications for the East Asian
352 summer monsoon. *Glob. Planet. Change* 121, 101–112.
- 353 Li, X.M., Wang, M.D., Zhang, Y.Z., Lei, L., Hou, J.Z., 2017a. Holocene climatic and environmental change
354 on the western Tibetan Plateau revealed by glycerol dialkyl glycerol tetraethers and leaf wax deuterium-
355 to-hydrogen ratios at Aweng Co. *Quat. Res.* 87, 455–467.
- 356 Li, Y., Qiang, M.R., Jin, Y.X., Liu, L., Zhou, A.F., Zhang, J.W., 2017b. Influence of aquatic plant
357 photosynthesis on the reservoir effect of Genggahai Lake, northeastern Qinghai-Tibetan Plateau.
358 *Radiocarbon* 60, 561–569.
- 359 Li, Y., Zhang, Y.X., Zhang, X.Z., Ye, W.T., Xu, L.M., Han, Q., Li, Y.C., Liu, H.B., Peng, S.M., 2020b. A
360 continuous simulation of Holocene effective moisture change represented by variability of virtual lake
361 level in East and Central Asia. *Sci. China-Earth Sci.* 63, 1161–1175.
- 362 Li, Z.F., Lv, J.F., 2001. Geomorphology, deposition and lake evolution of Dabusu Lake, Northeastern China.
363 *Journal of Lake Science*, 13, 103–110 (in Chinese).
- 364 Lister, G.S., Kelts, K.R., Chen, K.Z., Yu, J.Q., Niessen, F., 1991. Lake Qinghai, China: closed- basin lake
365 levels and the oxygen isotope record for ostracoda since the latest Pleistocene. *Paleogeogr. Paleoclimatol.*
366 *Paleoecol.* 84, 141–162.
- 367 Liu, X.J., Lai, Z.P., Madsen, D.B., Zeng, F.M., 2015. Last deglacial and Holocene lake level variations of
368 Qinghai Lake. *J. Quat. Sci.* 30, 245–257.
- 369 Lu, H.Y., Wu, N.Q., Liu, K.B., Zhu, L.P., Yang, X.D., Yao, T.D., Wang, L., Li, Q., Liu, X.Q., Shen, C.M., Li,
370 X.Q., Tong, G.B., Jiang, H., 2011. Modern pollen distributions in Qinghai-Tibetan Plateau and the
371 development of transfer functions for reconstructing Holocene environmental changes. *Quat. Sci. Rev.* 30,
372 947–966.
- 373 Mason, J.A., Lu, H., Zhou, Y., Miao, X., Swinehart, J.B., Liu, Z., Goble, R.J., Yi, S., 2009. Dune mobility and
374 aridity at the desert margin of northern China at a time of peak monsoon strength. *Geology* 37, 947–950.

375 Mischke, S., Zhang, C.J., Borner A, Herzsuh, U., 2010. Lateglacial and Holocene variation in aeolian
376 sediment flux over the northeastern Tibetan Plateau recorded by laminated sediments of a saline
377 meromictic lake. *J. Quat. Sci.* 25, 162–177.

378 Mishra, P.K., Ankit, Y., Gautam, P.K., Lakshmidivi, C.G., Singh, P., Anoop, A., 2019. Inverse relationship
379 between south-west and north-east monsoon during the late Holocene: Geochemical and sedimentological
380 record from Ennamangalam Lake, southern India. *Catena* 182, 104117.

381 Paillard, D., Labeyrie, L., Yiou, P., 1996. Macintosh program performs time-series analysis. *Eos, Transactions*
382 *American Geophysical Union*, 77, 379.

383 Pennington, W., 1979. The origin of pollen in lake sediments: an enclosed lake compared with one receiving
384 inflow streams. *New Phytol.* 83, 189–213.

385 Perrineau, A., van Der Woerd, J., Gaudemer, Y., Jing, L.-Z., Pik, R., Tapponnier, P., Thuizat, R., Zhang, Z.R.,
386 2011. Incision rate of the Yellow River in Northeastern Tibet constrained by ¹⁰Be and ²⁶Al cosmogenic
387 isotope dating of fluvial terraces: implications for catchment evolution and plateau building. *Geological*
388 *Society London Special Publication* 353, 189–219.

389 Prentice, I.C., Cramer, W., Harrison, S.P., Leemans, R., Monserud, R.A., Solomon, A.M., 1992. Special paper:
390 a global biome model based on plant physiology and dominance, soil properties and climate. *J. Biogeogr.*
391 117–134.

392 Qiang, M.R., Chen, F.H., Song, L., Liu, X.X., Li, M.Z., Wang, Q., 2013a. Late Quaternary aeolian activity in
393 Gonghe Basin, northeastern Qinghai-Tibetan plateau, China. *Quat. Res.* 79, 403–412.

394 Qiang, M.R., Jin, Y.X., Liu, X.X., Song, L., Li, H., Li, F.S., Chen, F.H., 2016. Late Pleistocene and Holocene
395 aeolian sedimentation in Gonghe Basin, northeastern Qinghai-Tibetan plateau: variability, processes, and
396 climatic implications. *Quat. Sci. Rev.* 132, 57–73.

397 Qiang, M.R., Song, L., Chen, F.H., Li, M.Z., Liu, X.X., Wang, Q., 2013b. A 16-kyr lake level record inferred
398 from macrofossils in a sediment core from Genggahai Lake, northeastern Qinghai-Tibetan Plateau
399 (China). *J. Paleolimn.* 49, 575–590.

400 Qiang, M.R., Song, L., Jin, Y. X., Li, Y., Liu, L., Zhang, J.W., Zhao, Y., Chen, F.H., 2017. A 16-kyroxygen-
401 isotope record from Genggahai Lake on the northeastern Qinghai-Tibetan Plateau: hydroclimatic
402 evolution and changes in atmospheric circulation. *Quat. Sci. Rev.* 162, 72–87.

403 Reimer, P.J., Baillie, M.G.L., Bard, E., Bayliss, A., Beck, J.W., Bertrand, C.J.H., Blackwell, P.G., Buck, C.E.,
404 Burr, G.S., Culter, K.B., Damon, P.E., Edwards, R.L., Fairbanks, R.G., Friedrich, M., Guilderson, T.P.,
405 Hogg, A.G., Hughen, K.A., Kromer, B., McCormac, G., Manning, S., Ramsey, C.B., Reimer, R.W.,
406 Remmele, S., Southon, J.R., Stuiver, M., Talamo, S., Taylor, F.W., van der Plicht, J., Weyhenmeyer, C.E.,
407 2009. IntCal09 and Marine09 radiocarbon age calibration curves, 0–50,000 years cal BP. *Radiocarbon* 51,
408 1111–1150.

409 Shen, J., Liu, X.Q., Wang, S.M., Matsumoto, R., 2005. Palaeoclimatic changes in the Qinghai Lake area
410 during the last 18,000 years. *Quat. Int.* 136, 131–140.

411 Walseng, B., 2016a. *Chydorus sphaericus* O.F.M. Artsdatabanken. Norwegian Institute of Environmental
412 Research. Available at <https://www.artsdatabanken.no/Pages/214507/>. Cited 27. September 2020.

413 Walseng, B., 2016b. *Alona rectangula* Sars. Artsdatabanken. Norwegian Institute of Environmental Research.
414 Available at <https://www.artsdatabanken.no/Pages/214487/>. Cited 27. September 2020.

415 Wang, Y.J., Cheng, H., Edwards, R.L., He, Y.Q., Kong, X.G., An, Z.S., Wu, J.Y., Kelly, M.J., Dykoski, C.A.,
416 Li, X.D., 2005. The Holocene Asian Monsoon: links to solar changes and North Atlantic Climate. *Science*
417 308, 854–857.

418 Webster, P.J., Magaña, V.O., Palmer, T.N., Shukla, J., Thomas, R.A., Yanai, M., Yasunari, T., 1998. Monsoons:
419 Processes, predictability, and the prospects for prediction. *J. Geophys. Res.-Atmos.* 103, 14451–14510.

420 Weckström, J., Korhola, A., Blom, T., 1997. The Relationship between Diatoms and Water Temperature in
421 Thirty Subarctic Fennoscandian Lakes. *Arct. Antarct. Alp. Res.* 29, 75–92.

422 Wei, H.C., E, C.Y., Zhang, J., Sun, Y.J., Li, Q.K., Hou, G.L., Duan, R.L., 2020. Climate change and
423 anthropogenic activities in qinghai lake basin over the last 8500 years derived from pollen and charcoal
424 records in an aeolian section. *Catena* 193, 104616.

425 Wen, R.L., Xiao, J.L., Chang, Z.G., Zhai, D.Y., Xu, Q.H., Li, Y.C., Itoh, S., Lomtatidze, Z., 2010. Holocene
426 climate changes in the mid-high-latitude-monsoon margin reflected by the pollen record from Hulun Lake,
427 northeastern Inner Mongolia. *Quat. Res.* 73, 293–303.

428 Wen, R.L., Xiao, J.L., Fan, J.W., Zhang, S.R., Yamagata, H., 2017. Pollen evidence for amid-Holocene East
429 Asian summer monsoon maximum in northern China. *Quat. Sci. Rev.* 176, 29–35.

430 Wilson, G.P., Reed, J.M., Frogley, M.R., Hughes, P.D., Tzedakis, P.C., 2015. Reconciling diverse lacustrine
431 and terrestrial system response to penultimate deglacial warming in southern Europe. *Geology* 43, 819–
432 822.

433 Wilson, L.R., 1941. The larger aquatic vegetation of Trout Lake, Vilas County, Wisconsin. *Transactions of the*
434 *Wisconsin Academy of Science Arts & Letters* 33, 135–146.

435 Xiao, J.L., Xu, Q.H., Nakamura, T., Yang, X.L., Liang, W.D., Inouchi, Y., 2004. Holocene vegetation
436 variation in the Daihai Lake region of north-central China: a direct indication of the Asian monsoon
437 climatic history. *Quat. Sci. Rev.* 23, 1669–1679

438 Zhang, M.M., Bu, Z.J., Wang, S.Z., Jiang, M., 2019. Moisture changes in Northeast China since the last
439 deglaciation: Spatiotemporal out-of-phase patterns and possible forcing mechanisms. *Earth-Sci. Rev.* 201,
440 102984.

441 Zhao, Y., Liu, Y.L., Guo, Z.T., Fang, K.Y., Li, Q., Cao, X.Y., 2017. Abrupt vegetation shifts caused by gradual
442 climate changes in central Asia during the Holocene. *Sci. China-Earth Sci.* 60, 1317–1327.

443 Zhou, T., Gong, D., Li, J., Li, B., 2009. Detecting and understanding the multi-decadal variability of the East
444 Asian summer monsoon recent progress and state of affairs. *Meteorol. Z.*, 18, 455–467.

445 **Figure and table captions**

446 **Fig. 1.** Location and modern environmental context of Genggahai Lake. (A) Overview map showing locations
447 of the paleoclimatic sites referenced in the text, and the dominant circulation systems of the westerlies and the
448 Asian monsoon. Genggahai Lake is indicated by a star. Lakes Qinghai (Shen et al., 2005), Kuhai (Mischke et
449 al., 2010), Dalianhai (Cheng et al., 2013), Gonghai (Chen et al., 2015), Chagan Nur (Li et al., 2020a), Dali
450 (Wen et al., 2017), Daihai (Xiao et al., 2004) and Hulun (Wen et al., 2010), Dabusu Lake (Li and Lv, 2001)
451 and Dongge Cave (Dykoski et al., 2005) are indicated by circles. The modern Asian summer monsoon limit is
452 shown by a green dashed line (after Gao et al., 1962). (B) Physical environment of the Gonghe Basin.
453 Mountain areas above 4,500 m a.s.l. and the potential catchment area of groundwater-fed Genggahai Lake are
454 delineated by the white dashed line and the blue dashed line (after Qiang et al., 2017), respectively. (C)
455 Vegetation (after Qiang et al., 2013b.) and coring sites.

456 **Fig. 2.** Records of plant macrofossils (A–F), Cladocera (G, H), and diatoms (I, J, K) from the sediments of
457 Genggahai Lake and the reconstructed lake level (L). (G, I, J) Relative abundance of Cladocera, planktonic
458 diatoms and non-planktonic diatoms, respectively. (H, K) Total counted individuals of Cladocera and diatoms,
459 respectively. In (A, C, E) green and red bars denote *Potamogeton pectinatus* (or *Myriophyllum spicatum*) and
460 *Chara* encrustations, respectively. Macrofossil stem encrustations are identified in the stratigraphy. *Chara*
461 gyrogonites are presented as individuals/dm² per year.

462 **Fig. 3.** Comparison of the synthesized tree pollen index (J, this study) and pollen records from the marginal
463 regions dominated by the ASM. (A, B) Total terrestrial pollen concentration from lakes Genggahai (this study)
464 and Qinghai (Shen et al., 2005), respectively. (C–I) Tree pollen percentages from lakes Genggahai (this study),
465 Qinghai (Shen et al., 2005), Dalianhai (Cheng et al., 2013), Gonghai (Chen et al., 2015), Dali (Wen et al.,
466 2017), Daihai (Xiao et al., 2004) and Hulun (Wen et al., 2010), respectively. The gray bar indicates the optimal
467 vegetation conditions during 8.6–6.9 cal kyr BP.

468 **Fig. 4.** Comparison of the lake-level record (A) and total terrestrial pollen concentration (I) from Genggahai
469 Lake and other paleoclimatic records. (B) Asian summer monsoon (ASM) index based on the sedimentary
470 carbonate and TOC content of the sediments of Qinghai Lake (An et al., 2012). (C) Simulated water level of
471 Qinghai Lake (Li et al., 2020b). (d) Mz (ϕ) grain-size record from Dabusu Lake (Li and Lv, 2001). (E, F)
472 Water level of Chagan Nur (Li et al., 2020a) and Dali Lake (Goldsmith et al., 2017), respectively. (G) Summer
473 insolation at 35°N (Berger and Loutre, 1991). (H) $\delta^{18}\text{O}_c$ record from Dongge Cave (Dykoski et al., 2005). (J)
474 Synthesized tree pollen index (this study). (K) Probability density plot of the OSL ages of eolian sand samples
475 from the NETP (Qiang et al., 2013a). (L) Synthesized sand percentages in eolian deposits in northeast China
476 (Li et al., 2014).

Title: Lateglacial and Holocene climate change in the NE Tibetan Plateau: Reconciling divergent proxies of Asian summer monsoon variability

DETAILED RESPONSES TO THE COMMENTS FROM REVIEWERS

Response to Reviewer #1:

The authors try to reconstruct the ASM since 15.4 ka based on some proxies. The attempt is encouraging. However, this version has some fundamental problems. Terrestrial proxy, pollen, is important in this manuscript. The authors indicate that sparse vegetation cover occurred during the early Holocene (11.3-8.4 cal kyr BP). Obviously, it is not correct. Fig. 3 shows that total terrestrial pollen concentrations and tree pollen percentages are highest on average in the whole sequence during 11-5.5 cal kyr BP. Thus, this period should occur relatively dense vegetation. The authors should reconsider how to reorganize the manuscript.

Thank you for your comments. We agree that the total terrestrial pollen concentrations and the tree pollen percentages are overall higher during 11.3-5.5 cal kyr BP, compared with the periods from 15.4 to 11.3 and from 5.5 to 0 cal kyr BP. However, the records further suggest that optimal vegetation conditions occurred during 8.6–6.9 cal kyr BP and that the terrestrial vegetation cover was relatively lower during the early Holocene (11.3–8.6 kyr cal BP), compared with the period from 8.6 to 6.9 kyr cal BP (see the figure below). This is clearly inconsistent with the aquatic biota inferred lake level record which shows the highest lake level during the early Holocene. This finding clearly reflects the existence of different hydroclimatic conditions between the lake and its catchment due to diverse driving mechanisms. We changed ‘sparse terrestrial vegetation during the early Holocene’ to ‘relatively lower vegetation cover during the early Holocene, compared with the period from 8.6 to 6.9 kyr cal BP’. In addition, we made small adjustments to the zonation of biota stratigraphy. See Fig. 2, 3 and 4, Lines 19-21, 25, 152, 157, 170-175, 220-221, 228-229, 235, 248-249, 256, 267, 275-280 (Line and figure number refers to the revised version in the responses).

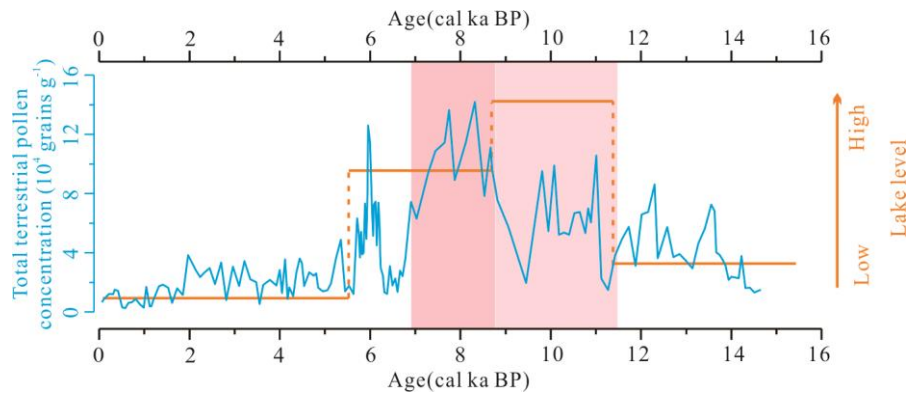


Fig. comparison of the lake level record and the total terrestrial pollen concentrations of Genggahai Lake

Response to Reviewer #2:

Li et al., presented a lake sediment record from the Asian monsoon-dominated area covering the late glacial and Holocene period focusing on the lake level fluctuations and terrestrial vegetation evolution to deeply understand the influences of the Asian summer monsoon to the lake and its catchment, especially during the early Holocene because they found distinct inconsistency derived from different proxies. I must declare that this is a manuscript which I have reviewed twice. In its first version, I found several major problems and the authors has revised a lot based on the comments from the reviewers and gave quite detailed responses and interpretations point by point which greatly improved the manuscript. I actually was satisfied with its revision and recommended publication.

I compared in details the current version to the previous one, there is only very minor changes therefore I have no any other major comments for this paper.

I think the interpretation of effective moisture which eventually influenced the vegetation development in the catchment were more convincing, it is a good idea to distinguish the different response to the precipitation/evaporation between lake and the catchment taking the infiltration process into account. Moreover, the discussion about the relationship between lake level changes and effective moisture within the catchment is much more detailed and this can give a more convincing mechanism behind the results included in the paper. In general, I believe the findings will be helpful to deeply understand the evolution of ASM during the early Holocene and its impact to the environment.

Thank you for your efforts to review this work. Your comments have greatly improved the manuscript. In the new version, We made small adjustments to the zonation of biota stratigraphy according to reviewer #1's comments, highlighting that a higher lake level and relatively lower terrestrial vegetation cover occurred synchronously during the early Holocene (11.3–8.6 kyr cal BP), compared with the

period from 8.6 to 6.9 kyr cal BP. See Fig. 2, 3 and 4.

Lateglacial and Holocene climate change in the NE Tibetan Plateau: Reconciling divergent proxies of Asian summer monsoon variability

Yuan Li^{a, c}, Mingrui Qiang^{b, c*}, Xiaozhong Huang^c, Yongtao Zhao^a, Jaakko J. Leppänen^d, Jan Weckström^d, Minna Väliranta^d

^a Key Laboratory of Desert and Desertification, Northwest Institute of Eco-Environment and Resources, Chinese Academy of Sciences, Lanzhou 730000, China.

^b School of Geography, South China Normal University, Guangzhou 510631, China

^c Key Laboratory of Western China's Environmental Systems (MOE), College of Earth and Environmental Sciences, Lanzhou University, Lanzhou 730000, China.

^d Environmental Change Research Unit, Ecosystems and Environment Research Programme and Helsinki Institute of Sustainability Science, Faculty of Biological and Environmental Sciences, P.O. Box 65, 00014 University of Helsinki, Finland.

Corresponding author: Mingrui Qiang (mrqiang@scnu.edu.cn).

Abstract

The nature of Holocene Asian summer monsoon (ASM) evolution documented by diverse natural archives remains controversial, with a contentious issue being whether or not a strong Asian summer monsoon prevailed during the early Holocene. Here we present sequences of multiple proxies measured in sediment cores from Genggahai Lake in the NE Tibetan Plateau (NETP). The results suggest that a higher lake level and relatively lower terrestrial vegetation cover occurred synchronously during the early Holocene (11.3–8.6 kyr cal BP), compared with the period from 8.6 to 6.9 kyr cal BP. This finding clearly reflects the existence of different hydroclimatic conditions between the lake and its catchment due to diverse driving mechanisms. The early Holocene high stand of the lake, as demonstrated by the stratigraphic variability of the remains of aquatic biota, may have responded to the strengthened ASM and increased monsoonal precipitation; the relatively low vegetation cover in the marginal region of the Asian monsoon during the early Holocene, and the coeval widespread active sand dune mobility in both the NE Tibetan Plateau and NE China, most likely resulted from a low level of effective moisture due to high evaporation, and hence they cannot be interpreted as evidence of a weak ASM. Our results potentially reconcile the current divergent interpretations of various proxy climate records from the region. Our findings suggest that the ASM evolution was characterized by a consistent pattern across the monsoonal regions, as indicated by the oxygen isotope record of Chinese speleothems.

33 *Key words:* Holocene; monsoon; China; Micropaleontology; lake level; vegetation.

34 **1 Introduction**

35 The Asian monsoon system affects more than half of the world's population and the
36 associated ecosystems (Webster et al., 1998). Understanding the variability of the Asian
37 monsoon has significant implications for the social and ecological systems in the region (Hansen
38 and Lebedeff, 1987; Mishra et al., 2019). Precipitation in the marginal regions dominated by the
39 Asian summer monsoon (ASM) is highly dependent on the strength of the ASM: a stronger ASM
40 circulation can transport more water vapor, leading to higher precipitation, and vice versa (Zhou
41 et al., 2009). Therefore, precipitation in these marginal regions can directly reflect the strength of
42 the ASM (Chen et al., 2015). Over the past two decades, numerous studies of the Holocene
43 evolution of the ASM have been conducted based on diverse natural archives from the region
44 (e.g., Chen et al., 2015; Dykoski et al., 2005; Goldsmith et al., 2017; Hu et al., 2008; Li et al.,
45 2014; Wang et al., 2005; Wei et al., 2020). However, the nature of ASM evolution during the
46 Holocene still remains controversial, with a contentious issue being whether or not a strong
47 Asian summer monsoon prevailed during the early Holocene. For example, the early Holocene
48 high-stand of lakes in the marginal regions dominated by the ASM (Fig. 1A), including lakes
49 Dali (Goldsmith et al., 2017), Dabusu (Li and Lv, 2001) and Kuhai (Mischke et al., 2010),
50 reflects an intensified ASM which is consistent with monsoonal records from Chinese
51 speleothems (Dykoski et al., 2005; Hu et al., 2008; Wang et al., 2005). However, records of
52 pollen assemblages and/or pollen-based precipitation from the lakes in the region (Fig. 1A),
53 including lakes Gonghai (Chen et al., 2015), Dalianhai (Cheng et al., 2013), Daihai (Xiao et al.,
54 2004), Dali (Wen et al., 2017) and Hulun (Wen et al., 2010), together with evidence for
55 widespread sand dune mobility in NE China (Li et al., 2014), indicate the occurrence of dry
56 terrestrial conditions at this time, possibly related to a weak ASM. Furthermore, even diverse
57 proxies generated from the same study site may exhibit divergent patterns of Holocene climate
58 change and ASM evolution. For example, at Qinghai Lake, the geochemical proxies (An et al.,
59 2012; Jin et al., 2015; Lister et al., 1991) generally suggest a high lake level and a strong ASM
60 during the early Holocene. In contrast, the shoreline deposits (Liu et al., 2015) and the pollen
61 assemblages (Shen et al., 2005) suggest that the lake level probably was low at this time, induced
62 by high evaporation or a weak ASM. These seemingly contradictory interpretations, especially
63 those from the same site (e.g., Qinghai Lake), cannot be explained by the spatial and temporal
64 differentiation of ASM evolution, or by chronological uncertainties. Therefore, a comprehensive
65 analysis of the driving mechanisms of these proxies and their linkage to the ASM are essential
66 for reconciling the controversy.

67 Genggahai Lake is a small, shallow lake in the NE Tibetan Plateau (NETP) (Fig. 1A),
68 located in the marginal region dominated by the ASM. The sediments are rich in the remains of
69 aquatic biota and terrestrial pollen, which provide the opportunity to conduct multi-proxy
70 investigations of ASM evolution. Qiang et al. (2013b) have discussed the lake-level fluctuations
71 over the past 16 kyr based mainly on plant macrofossil assemblages in the sediments from a
72 single core (GGH-A) recovered from the lake. However, the early Holocene high-stand of the
73 lake was indirectly inferred by geochemical variables (total organic carbon, total nitrogen and
74 carbon isotopic composition of bulk sediment organic matter), due to the absence of plant
75 macrofossils (Qiang et al., 2013b). In addition, the evolution of lake bathymetry may also lead to
76 lake-level fluctuations on a long timescale (Hilton, 1985; Lehman, 1975), which was not
77 differentiated from the influence of climatic factors in the previous study (Qiang et al., 2013b).
78 Therefore, comprehensive analyses of diverse bioindicators (e.g., plant macrofossils, Cladocera,
79 diatoms) from multiple cores are essential not only for the reliable reconstruction of lake-level
80 fluctuations, but also for assessing the influence of the evolution of lake bathymetry on the lake-
81 level fluctuations, and for understanding regional hydroclimatic changes (Dearing, 1997).
82 Moreover, the evolution of the regional terrestrial vegetation and its potential linkages to the
83 ASM remain unclear.

84 Here we present sequences of aquatic (plant macrofossils, Cladocera, diatoms) and
85 terrestrial (terrestrial pollen) proxies derived from multiple sediment cores from Genggahai
86 Lake. Combined with hydrological and ecological investigations of the modern lake, and with
87 reference to independent climatic records from the marginal regions dominated by the ASM, our
88 aims were to reconstruct the regional ASM variability during the Lateglacial and the Holocene,
89 and to reconcile the current divergent results of proxy indicators of ASM evolution.

90 **2 Materials and Methods**

91 Genggahai Lake (36°11'N, 100°06'E) is located in the central Gonghe Basin (Fig. 1B) at
92 an altitude of 2,860 m a.s.l. The lake is small (surface area, ~2 km²) and shallow (maximum
93 water depth, ~1.8 m) and has an elevated salinity (~1.2 g L⁻¹) and pH (~9.1). *Potamogeton*
94 *pectinatus*, *Myriophyllum spicatum*, and *Chara* spp. dominate the submerged macrophyte
95 communities in the current lake. The lake is mainly fed by groundwater. Several small spring-
96 water streams flow into the lake. Three sediment cores were recovered from Genggahai Lake in
97 January 2008 and January 2013 using a modified Livingstone piston corer. Cores GGH-A (length
98 782 cm) and GGH-C (length 774 cm) were recovered from the center of the lake in a water depth
99 of 170 cm (Fig. 1C), and core GGH-E (length 765 cm) was recovered from the northwest littoral
100 area in a water depth of 110 cm (Fig. 1C). Due to the lack of terrestrial plant remains, samples of

101 the leaves of aquatic macrophytes were picked from the sediments for accelerator mass
102 spectrometry (AMS) ^{14}C dating, conducted by Beta Analytic Inc. (Miami, USA) (Table S1). The
103 reservoir age of the lake was estimated at 1,010 ^{14}C years on average, based on the AMS ^{14}C
104 dating results of the dissolved inorganic carbon of the lake water, macrophyte remains in the
105 lake's surface sediments and living *P. pectinatus* (Li et al., 2017b). A total of 26 ^{14}C ages from
106 cores GGH-A (cited from Qiang et al. 2013b), GGH-C, and GGH-E (Table S1), which are in
107 stratigraphic order, were calibrated to calendar years (Calib 6.0.1, Reimer et al., 2009) after
108 subtracting an average reservoir age (1,010 yr). The age-depth models of the three cores were
109 generated by the Bacon Bayesian age-modeling software (Blaauw and Christen, 2011), using the
110 calibrated radiocarbon ages. The age versus depth profiles of the three cores agree well with each
111 other, which supports their reliability (Fig. S1).

112 Plant macrofossils, including *Chara* gyrogonites (Fig. 2B, 2D, 2F) and encrustations of
113 *Chara* spp. and *P. pectinatus* (or *M. spicatum*) (Fig. 2A, 2C, 2E), were picked from cores GGH-
114 A (cited from Qiang et al. 2013b), GGH-C, and GGH-E. Cladocera (Fig. 2G) and diatom (Fig. 2I,
115 2G) analyses were conducted on core GGH-C using standard methods (Korhola and Rautio,
116 2001; Weckström et al., 1997). In addition, fossil pollen (Fig. 3A, 3C) was extracted from core
117 GGH-A following the methods of Fægri and Iversen (1989). In order to comprehensively depict
118 the terrestrial vegetation conditions in the marginal regions dominated by the ASM, we compiled
119 six lacustrine tree pollen records from the region, including from lakes Qinghai (Shen et al.,
120 2005), Dalianhai (Cheng et al., 2013), Gonghai (Chen et al., 2015), Dali (Wen et al., 2017),
121 Daihai (Xiao et al., 2004) and Hulun (Wen et al., 2010). Since the changes in the tree pollen
122 content of these records show a similar trend, a synthesized tree pollen index covering the past
123 12 kyr (obtained by taking the average of the normalized tree pollen contents from the six lakes)
124 was used to portray changes in tree cover in the marginal regions dominated by the ASM
125 (Fig. 3). Further details about the method are given in the supplements.

126 **3 Results and discussion**

127 3.1. Patterns of hydroclimatic evolution indicated by lake level and pollen sequences

128 In general, submerged macrophytes, Cladocera, and diatoms in freshwater lakes are
129 sensitive to changes in water level, and thus their fossil remains in lake sediments can be used to
130 reconstruct past water-level fluctuations (Birks, 1993; Heggen et al., 2012). The aquatic plant
131 macrofossils in the sediments of Genggahai Lake mainly originate from *Chara* spp.,
132 *P. pectinatus* and *M. spicatum*. These species also dominate the lake today and they are common
133 in shallow lakes worldwide (Wilson et al., 1941). The spatial distribution of submerged
134 macrophytes in the modern lake is mainly modulated by the water depth, and the shallow water

135 zone of the lake is occupied by *Chara* spp. (Fig. S2) (Qiang et al., 2013b). Therefore, the
136 occurrence of the fossil remains of *Chara* spp. and *P. pectinatus* (or *M. spicatum*) in the lake
137 sediments, especially the occurrence of abundant *Chara* gyrogonites, most likely reflects a
138 shallow water environment. As for fossil Cladocera, only two littoral species (*Chydorus*
139 *sphaericus* and *Coronatella rectangula*) which prefer macrophyte habitats were identified in the
140 sediments of Lake Genggahai (Walseng, B., 2016a, 2016b). Diatoms in the sediments are
141 relatively diverse, consisting of both planktonic (e.g., *Lindavia comta* and *Cyclotella*
142 *distinguenda*) and non-planktonic species (e.g., *Gomphonema angustum* and *Achnanthes*
143 *minutissima*). Based on changes in submerged macrophytes, Cladocera and diatoms in the lake
144 sediments (Fig. 2), the history of lake-level fluctuations was divided into the following four
145 stages:

146 **15.4–11.3 cal kyr BP** The lake sediments contain abundant submerged-macrophyte
147 encrustations, *Chara* gyrogonites and littoral cladoceran fossils, reflecting a shallow lake. In
148 addition, the diatom assemblages are dominated by both planktonic (e.g., *L. comta* and *C.*
149 *distinguenda*) and non-planktonic species (e.g., *G. angustum*). Notably, *C. distinguenda* is a
150 *tychoplanktonic species* which can adapt to shallow water conditions. Therefore, the lake level
151 most likely was low during this period.

152 **11.3–8.6 cal kyr BP** Submerged macrophytes and Cladocera largely disappear from the
153 sediments. In addition, the diatom assemblages are dominated by an euplanktonic species (i.e., *L.*
154 *comta*). Thus we conclude that the lake level was high during this period, and it may have
155 exceeded the depth limit for submerged macrophytes, resulting in the absence of Cladocera
156 macrophyte habitats and increasing the abundance of planktonic diatoms.

157 **8.6–5.5 cal kyr BP** Submerged macrophyte encrustations occur episodically and *Chara*
158 gyrogonites are relatively scarce. Cladocera fossils largely disappear from the sediments,
159 probably in response to the scarcity of macrophyte habitats. The diatom assemblages are
160 dominated by both planktonic (e.g., *L. comta* and *C. distinguenda*) and non-planktonic species.
161 Thus we conclude that the lake level during this period was probably high overall, but lower than
162 during the previous stage.

163 **5.5 kyr cal BP to the present** The lake sediments contain abundant submerged-
164 macrophyte encrustations, *Chara* gyrogonites, littoral Cladocera fossils, and non-planktonic
165 diatoms, reflecting a shallow lake.

166 The terrestrial pollen in lake sediments is mainly derived from the catchment and hence it
167 reflects the local and regional terrestrial vegetation conditions (Pennington, 1979). Changes in
168 total terrestrial pollen concentrations (Fig. 3A) and tree pollen contents (Fig. 3C) in the

169 sediments of Genggahai Lake are largely in agreement with those at nearby Qinghai Lake (Fig.
170 3B, 3D) and the synthesized tree pollen index (Fig. 3J), showing that optimal vegetation
171 conditions occurred during 8.6–6.9 cal kyr BP. Overall, the aquatic and animal fossils
172 (macrophytes, Cladocera, diatoms) and terrestrial pollen in the sediments of Genggahai Lake
173 indicate that a higher lake level and relatively lower terrestrial vegetation cover occurred
174 synchronously during the early Holocene (11.3–8.6 kyr cal BP), compared with the period from
175 8.6 to 6.9 kyr cal BP. This implies the occurrence of different hydroclimatic conditions between
176 the lake and its catchment (Fig. 4A, 4I). This apparent contradiction is also reflected in proxy
177 sequences from other lakes in the marginal regions dominated by the ASM: e.g., at Lakes
178 Qinghai (An et al., 2012; Shen et al., 2005), Dali (Goldsmith et al., 2017; Wen et al., 2017) and
179 Chagan Nur (Li et al., 2020a).

180 3.2. Implications for the evolution of the Asian summer monsoon

181 The early Holocene high lake levels and low total pollen concentrations (or tree
182 percentages) recorded by lake sediments from the margins of the regions dominated by the ASM
183 are mutually contradictory in terms of their interpretation as evidence for ASM strength (e.g., An
184 et al., 2012; Chen et al., 2015), or as evidence for the spatial differentiation of ASM evolution
185 (Zhang et al., 2019). However, these seemingly contradictory patterns most likely reflect the
186 existence of different hydroclimatic conditions between the lake and its catchment due to diverse
187 driving mechanisms (cf., Wilson et al., 2015), and they cannot simultaneously be interpreted as
188 proxies of ASM strength.

189 In general, lake-level fluctuations are controlled by the water balance of the lake.
190 However, previous studies have demonstrated that the evolution of lake bathymetry on a long
191 timescale may also result in lake-level fluctuations (Hilton, 1985; Lehman, 1975). Increased
192 allochthonous input of detrital materials will enhance the sedimentation rate in the deepest parts
193 of the lake due to gravity (i.e., the “sediment-focusing effect”) which will lead to decreases in
194 water depth (Hilton, 1985). However, at Genggahai Lake, the AMS ¹⁴C dating results show that
195 the sedimentation rate of the central cores (GGH-A and GGH-C) was largely consistent with that
196 of the littoral core (GGH-E) during the Lateglacial and Holocene (Fig. S1), indicating that
197 changes in lake bathymetry since the Lateglacial were probably minor, exerting little effect on
198 the lake level. This could be ascribed to the flat lake basin morphometry and the dense growth of
199 submerged macrophytes, which largely restricted re-suspension and transport of sediments to the
200 depocenter (cf. Dearing, 1997). Therefore, lake-level fluctuations mainly represent the balance
201 between water inflows and losses. Currently, there are no large glaciers on the summits of the
202 mountains surrounding Genggahai Lake. In addition, the Lateglacial glaciers on these mountains

203 were mainly distributed in areas above 4,500 m a.s.l. (Fig. 1B) (Li et al., 1991) and therefore
204 their total extent was relatively small. Thus they are unlikely to have continuously contributed
205 meltwater which could sustain the high lake level during the early Holocene (11.3–8.6 cal kyr
206 BP), given the temperature increase of ~3 °C at the onset of the Holocene (Herzschuh et al., 2014;
207 Li et al., 2017a). Genggahai Lake is fed mainly by groundwater. Loose, porous fluvio-lacustrine
208 sediments of the Gonghe Formation (Perrineau et al., 2011) and surficial fluvial-fan sediments
209 largely constitute the catchment substrate of groundwater. In addition, the deep incision of the
210 Yellow River in the eastern Gonghe Basin led to a steep hydraulic gradient of the basin
211 (Craddock et al., 2010). Therefore, the catchment of groundwater was highly permeable, and
212 hence precipitation can infiltrate rapidly into the ground and feed the lake. The evaporation
213 losses during the infiltration process were most likely low. In addition, the catchment area of the
214 groundwater feeding the lake is far larger than the lake's surface area (Fig. 1B). Therefore,
215 evaporation may play a minor role in the water balance of the lake, and hence the lake-level
216 fluctuations can be interpreted as indicating changes in regional precipitation, reflecting the
217 strength of the ASM in the study area. The pattern of water-level fluctuations at Genggahai Lake
218 largely coincides with that of other lakes in the marginal regions dominated by the ASM (e.g.,
219 Qinghai, Kuhai, Dali, Dabusu and Chagan Nur) (Fig. 4B–F). This consistent pattern suggests a
220 weak ASM during 15.4–11.3 cal kyr BP, a significantly intensified ASM during 11.3–8.6 cal
221 kyr BP, and a gradually weakening ASM thereafter. In addition, the results of a modeling study
222 of water level changes at Qinghai Lake also reveal an early Holocene high-stand (Fig. 4C) (Li et
223 al., 2020b).

224 The evolution of terrestrial vegetation is generally the integrated reactions to multiple
225 environmental factors, including temperature, precipitation and the available water capacity of
226 the soil (Prentice et al., 1992). The sparse terrestrial vegetation in the marginal regions
227 dominated by the ASM during 15.4–11.3 cal kyr BP and 5.5–0 cal kyr BP mainly resulted from
228 low monsoonal precipitation and low temperatures (Lu et al., 2011). In addition, the relatively
229 low total terrestrial pollen concentration (Fig. 4I) during the early Holocene (11.3–8.6 kyr cal BP)
230 suggests that the terrestrial vegetation did not respond to the significantly ameliorated
231 environmental conditions, although the monsoonal precipitation increased sharply. Significantly,
232 changes in terrestrial vegetation are modulated mainly by effective moisture rather than by
233 precipitation (Prentice et al., 1992). Furthermore, changes in effective moisture do not always
234 respond linearly to variations in precipitation, but rather they depend on the balance between
235 precipitation and evaporation. Therefore, the relatively low terrestrial vegetation cover in the
236 study area during the early Holocene mostly likely reflects a low level of effective moisture.
237 Notably, the low effective moisture during this interval is also documented by the widespread

238 sand dune mobility in both the NETP and NE China (Fig. 4K, 4L) (Li et al., 2014; Qiang et al.,
239 2013a). Given that the enhanced monsoonal precipitation during the early Holocene may have
240 infiltrated rapidly into the ground due to the porous nature of the soils and the steep hydraulic
241 gradient of the catchment, the water retained in the soils probably could not compensate for the
242 intense evaporation loss as a consequence of the high temperatures (Li et al., 2017a) and high
243 summer insolation. This may have led to a low level of effective moisture and further restricted
244 the development of both the terrestrial vegetation and paleosols (Mason et al., 2009; Qiang et al.,
245 2013a, 2016). In addition, the strong ASM during this period would have resulted in the strong
246 release of latent heat by water (Herzschuh et al., 2014), which may have further increased
247 temperatures and evaporation. By contrast, decreased temperatures (Li et al., 2017a), due to the
248 reduction in both summer insolation and release of latent heat by water vapor during the period
249 from 8.6 to 6.9 cal kyr BP, likely resulted in the weakened evaporation of soil water and hence
250 led to the widespread development of vegetation (Fig. 3) and palaeosols (Li et al., 2014; Qiang et
251 al., 2013a) in the marginal regions dominated by the ASM. In addition, given that the terrestrial
252 vegetation has a lagged response to precipitation changes, the different response rates of the lake
253 water and terrestrial vegetation to climate change may also have contributed to the occurrence of
254 different hydroclimatic conditions between Genggahai Lake and its catchment (Zhao et al.,
255 2017).

256 The diverse proxies derived from sediments of Genggahai Lake clearly reveal the
257 synchronous occurrence of high lake levels and relatively low terrestrial vegetation cover, which
258 are correlative with evidence for widespread sand dune mobility in the marginal regions
259 dominated by the ASM during the early Holocene. These features do not reflect different
260 climatic patterns, but rather they reflect different aspects of monsoonal climate change. The
261 consistent high-stand of the lakes from these monsoon margin areas suggests increased
262 monsoonal precipitation during the early Holocene, providing compelling evidences for the
263 spatial consistency of ASM evolution documented by oxygen isotopic records from Chinese cave
264 deposits (Cheng et al., 2019; Dykoski et al., 2005; Hu et al., 2008; Wang et al., 2005). The strong
265 ASM and the increased monsoonal precipitation in the marginal regions dominated by the ASM
266 during the early Holocene are ascribed to the enhanced thermal contrast between land and sea in
267 spring and summer due to the increased orbitally-induced summer insolation (Fig. 4G, 4H). The
268 relatively low terrestrial vegetation cover during the early Holocene, as well as the widespread
269 dune sands in eolian sections in both the NETP and NE China, most likely reflect low effective
270 moisture conditions due to high evaporation, and hence they cannot be interpreted as evidence of
271 a weak monsoon.

272 **4 Conclusions**

273 The water-level fluctuations of Genggahai Lake and the vegetation conditions in its
274 catchment were reconstructed from the aquatic biota and pollen preserved in the lake sediments.
275 The results suggest a higher lake level and a stronger ASM during 11.3–5.5 cal kyr BP,
276 compared to the intervals of 15.4–11.3 cal kyr BP and 5.5–0 cal kyr BP. However, the total
277 terrestrial pollen concentration indicates relatively lower terrestrial vegetation cover during the
278 early Holocene (11.3–8.6 cal kyr BP), compared with the period from 8.6 to 6.9 kyr cal BP. In
279 contrast to the lake-level fluctuations, the vegetation cover in the catchment cannot be used as a
280 proxy for variations in monsoonal precipitation and thus ASM strength. Rather, the relatively
281 low vegetation cover mainly reflects a low level of effective moisture conditions, as a result of
282 intense evaporation due to high temperatures during the early Holocene.

283 **Declaration of Competing Interest**

284 The authors declare that they have no known competing financial interests or personal
285 relationships that could have appeared to influence the work reported in this paper.

286 **Acknowledgments**

287 We thank Dr. J. Bloemendal for his helpful comments and language improvements. This
288 research was supported by the National Natural Science Foundation of China (grants 41901103,
289 41671190, 41271219 and 41807440), the National Key R&D Program of China (grant
290 2017YFA0603402), and the Foundation for Excellent Youth Scholars of the “Northwest Institute
291 of Eco-Environment and Resources”, CAS.

292 **References**

- 293 An, Z.S., Colman, S.M., Zhou, W.J., Li, X.Q., Brown, E.T., Timothy Jull, A.J., Cai, Y.J., Huang, Y.S., Lu,
294 X.F., Chang, H., Song, Y.G., Sun, Y.B., Xu, H., Liu, W.G., Jin, Z.D., Liu, X.D., Cheng, P., Liu, Y., Ai, L.,
295 Li, X.Z., Liu, X.J., Yan, L.B., Shi, Z.G., Wang, X.L., Wu, F., Qiang, X.K., Dong, J.B., Lu, F.Y., Xu,
296 X.W., 2012. Interplay between the Westerlies and Asian monsoon recorded in Lake Qinghai sediments
297 since 32 ka. *Sci. Rep.* 2, 619–625.
- 298 Berger, A., Loutre, M.F., 1991. Isolation values for the climate of the last 10 million years. *Quat. Sci. Rev.* 10,
299 297–317.
- 300 Birks, H.H., 1993. The importance of plant macrofossils in late glacial climatic reconstructions: an example
301 from western Norway. *Quat. Sci. Rev.* 12, 719–726.
- 302 Blaauw, M., Christen, J.A., 2011. Flexible paleoclimate age depth models using an autoregressive gamma
303 process. *Bayesian Anal.* 6, 457–474.

304 Chen, F.H., Xu, Q.H., Chen, J.H., Birks, H.J., Liu, J.B., Zhang, S.R., Jin, L., An, C.B., Telford, R.J., Cao, X.Y.,
305 Wang, Z.L., Zhang, X.J., Selvaraj, K., Lu, H.Y., Li, Y.C., Zheng, Z., Wang, H.P., Zhou, A.F., Dong, G.H.,
306 Zhang, J.W., Huang, X.Z., Bloemendal, J., Rao, Z.G., 2015. East Asian summer monsoon precipitation
307 variability since the last deglaciation. *Sci. Rep.* 5, 11186.

308 Cheng, B., Chen, F.H., Zhang, J.W., 2013. Palaeovegetational and palaeoenvironmental changes since the last
309 deglacial in Gonghe Basin, northeast Tibetan Plateau. *J. Geogr. Sci.* 23, 136–146.

310 Cheng, H., Zhang, H.W., Zhao, J.Y., Li, H.Y., Ning, Y.F., Kathayat, G., 2019. Chinese stalagmite
311 paleoclimate researches: A review and perspective. *Sci. China-Earth Sci.* 62, 1489–1513.

312 Craddock, W.H., Kirby, E., Harkins, N.W., Zhang, H.P., Shi, X.H., Liu, J.H., 2010. Rapid fluvial incision
313 along the Yellow River during headwater basin integration. *Nat. Geosci.* 3, 209–213.

314 Dearing, J.A., 1997. Sedimentary indicators of lake-level changes in the humid temperate zone: a critical
315 review. *J. Paleolimn.* 18, 1–14.

316 Dykoski, C.A., Edwards, R.L., Cheng, H., Yuan, D.X., Cai, Y.J., Zhang, M.L., Lin, Y.S., Qing, J.M., An, Z.S.,
317 Revenaugh, J., 2005. A high-resolution, absolute-dated Holocene and deglacial Asian monsoon record
318 from Dongge Cave, China. *Earth Planet. Sci. Lett.* 233, 71–86.

319 Fægri, K., Iversen, J., 1989. *Textbook of Pollen Analysis*, fourth ed. John Wiley & Sons, Chichester.

320 Gao, Y.X., Xu, S.Y., Guo, Q.Y., Zhang, M.L., 1962. Monsoon regions in China and regional climates. In: Gao,
321 Y.X. (Ed.), *Some Problems on East-Asia Monsoon*. Science Press, Beijing, pp. 49–63 (in Chinese).

322 Goldsmith, Y., Broecker, W.S., Xu, H., Polissar, P.J., deMenocal, P.B., Porat, N., Lan, J.H., Cheng, P., Zhou,
323 W.J., An, Z.S., 2017. Northward extent of East Asian monsoon covaries with intensity on orbital and
324 millennial timescales. *Proc. Natl. Acad. Sci.* 114, 1817–1821.

325 Hansen, J., Lebedeff, S., 1987. Global trends of measured surface air temperature. *J. Geophys. Res.-Atmos.* 92,
326 13345–13372.

327 Heggen, M.P., Birks, H.H., Heiri, O., Grytnes, J.A., Birks, H.J.B., 2012. Are fossil assemblages in a single
328 sediment core from a small lake representative of total deposition of mite, chironomid, and plant
329 macrofossil remains? *J. Paleolimn.* 48, 669–691.

330 Herzsuh, U., Borkowski, J., Schewe, J., Mischke, S., Tian, F., 2014. Moisture advection feedback supports
331 strong early-to-mid Holocene monsoon climate on the eastern Tibetan Plateau as inferred from a pollen-
332 based reconstruction. *Paleogeogr. Paleoclimatol. Paleoecol.* 402, 44–54.

333 Hilton, J.A., 1985. Conceptual framework for predicting the occurrence of sediment focusing and sediment
334 redistribution in small Lakes. *Limnol. Oceanogr.* 30, 1131–1143.

335 Hu, C.Y., Henderson, G.M., Huang, J.H., Xie, S.C., Sun, Y., Johnson, K.R., 2008. Quantification of Holocene
336 Asian monsoon rainfall from spatially separated cave records. *Earth Planet. Sci. Lett.* 266, 221–232.

337 Jin, Z.D., An, Z.S., Yu, J.M., Li, F.C., Zhang, F., 2015. Lake Qinghai sediment geochemistry linked to
338 hydroclimate variability since the last glacial. *Quat. Sci. Rev.* 122, 63–73.

- 339 Korhola, A., Rautio, M., 2001. Cladocera and other Branchiopod crustaceans. In: Smol, J.P., Birks, J.B., Last,
340 W.M. (Eds.), Tracking environmental change using lake sediments. Zoological indicators. Kluwer,
341 Dordrecht. pp. 5–41.
- 342 Lehman, J.T., 1975. Reconstructing the rate of accumulation of lake sediment: The effect of sediment focusing.
343 *Quat. Res.* 5, 541–550.
- 344 Li, G.Q., Wang, Z., Zhao, W.W., Jin, M., Wang, X.Y., Tao, S.X., Chen, C.Z., Cao, X.Y., Zhang, Y.N., Yang,
345 H., Madsen, D., 2020a. Quantitative precipitation reconstructions from Chagan Nur revealed lag response
346 of East Asian summer monsoon precipitation to summer insolation during the Holocene in arid northern
347 China. *Quat. Sci. Rev.* 239, 106365.
- 348 Li, J.J., Zhou, S.Z., Pan, B.T., 1991. The problems of Quaternary glaciation in the eastern part of Qinghai-
349 Xizang Plateau. *Quaternary Sciences* 3, 193–203 (in Chinese with English abstract).
- 350 Li, Q., Wu, H.B., Yu, Y.Y., Sun, A.Z., Markovic, S.B., Guo, Z.T., 2014. Reconstructed moisture evolution of
351 the deserts in northern China since the Last Glacial Maximum and its implications for the East Asian
352 summer monsoon. *Glob. Planet. Change* 121, 101–112.
- 353 Li, X.M., Wang, M.D., Zhang, Y.Z., Lei, L., Hou, J.Z., 2017a. Holocene climatic and environmental change
354 on the western Tibetan Plateau revealed by glycerol dialkyl glycerol tetraethers and leaf wax deuterium-
355 to-hydrogen ratios at Aweng Co. *Quat. Res.* 87, 455–467.
- 356 Li, Y., Qiang, M.R., Jin, Y.X., Liu, L., Zhou, A.F., Zhang, J.W., 2017b. Influence of aquatic plant
357 photosynthesis on the reservoir effect of Genggahai Lake, northeastern Qinghai-Tibetan Plateau.
358 *Radiocarbon* 60, 561–569.
- 359 Li, Y., Zhang, Y.X., Zhang, X.Z., Ye, W.T., Xu, L.M., Han, Q., Li, Y.C., Liu, H.B., Peng, S.M., 2020b. A
360 continuous simulation of Holocene effective moisture change represented by variability of virtual lake
361 level in East and Central Asia. *Sci. China-Earth Sci.* 63, 1161–1175.
- 362 Li, Z.F., Lv, J.F., 2001. Geomorphology, deposition and lake evolution of Dabusu Lake, Northeastern China.
363 *Journal of Lake Science*, 13, 103–110 (in Chinese).
- 364 Lister, G.S., Kelts, K.R., Chen, K.Z., Yu, J.Q., Niessen, F., 1991. Lake Qinghai, China: closed- basin lake
365 levels and the oxygen isotope record for ostracoda since the latest Pleistocene. *Paleogeogr. Paleoclimatol.*
366 *Paleoecol.* 84, 141–162.
- 367 Liu, X.J., Lai, Z.P., Madsen, D.B., Zeng, F.M., 2015. Last deglacial and Holocene lake level variations of
368 Qinghai Lake. *J. Quat. Sci.* 30, 245–257.
- 369 Lu, H.Y., Wu, N.Q., Liu, K.B., Zhu, L.P., Yang, X.D., Yao, T.D., Wang, L., Li, Q., Liu, X.Q., Shen, C.M., Li,
370 X.Q., Tong, G.B., Jiang, H., 2011. Modern pollen distributions in Qinghai-Tibetan Plateau and the
371 development of transfer functions for reconstructing Holocene environmental changes. *Quat. Sci. Rev.* 30,
372 947–966.
- 373 Mason, J.A., Lu, H., Zhou, Y., Miao, X., Swinehart, J.B., Liu, Z., Goble, R.J., Yi, S., 2009. Dune mobility and
374 aridity at the desert margin of northern China at a time of peak monsoon strength. *Geology* 37, 947–950.

375 Mischke, S., Zhang, C.J., Borner A, Herzsuh, U., 2010. Lateglacial and Holocene variation in aeolian
376 sediment flux over the northeastern Tibetan Plateau recorded by laminated sediments of a saline
377 meromictic lake. *J. Quat. Sci.* 25, 162–177.

378 Mishra, P.K., Ankit, Y., Gautam, P.K., Lakshmidivi, C.G., Singh, P., Anoop, A., 2019. Inverse relationship
379 between south-west and north-east monsoon during the late Holocene: Geochemical and sedimentological
380 record from Ennamangalam Lake, southern India. *Catena* 182, 104117.

381 Paillard, D., Labeyrie, L., Yiou, P., 1996. Macintosh program performs time-series analysis. *Eos, Transactions*
382 *American Geophysical Union*, 77, 379.

383 Pennington, W., 1979. The origin of pollen in lake sediments: an enclosed lake compared with one receiving
384 inflow streams. *New Phytol.* 83, 189–213.

385 Perrineau, A., van Der Woerd, J., Gaudemer, Y., Jing, L.-Z., Pik, R., Tapponnier, P., Thuizat, R., Zhang, Z.R.,
386 2011. Incision rate of the Yellow River in Northeastern Tibet constrained by ¹⁰Be and ²⁶Al cosmogenic
387 isotope dating of fluvial terraces: implications for catchment evolution and plateau building. *Geological*
388 *Society London Special Publication* 353, 189–219.

389 Prentice, I.C., Cramer, W., Harrison, S.P., Leemans, R., Monserud, R.A., Solomon, A.M., 1992. Special paper:
390 a global biome model based on plant physiology and dominance, soil properties and climate. *J. Biogeogr.*
391 117–134.

392 Qiang, M.R., Chen, F.H., Song, L., Liu, X.X., Li, M.Z., Wang, Q., 2013a. Late Quaternary aeolian activity in
393 Gonghe Basin, northeastern Qinghai-Tibetan plateau, China. *Quat. Res.* 79, 403–412.

394 Qiang, M.R., Jin, Y.X., Liu, X.X., Song, L., Li, H., Li, F.S., Chen, F.H., 2016. Late Pleistocene and Holocene
395 aeolian sedimentation in Gonghe Basin, northeastern Qinghai-Tibetan plateau: variability, processes, and
396 climatic implications. *Quat. Sci. Rev.* 132, 57–73.

397 Qiang, M.R., Song, L., Chen, F.H., Li, M.Z., Liu, X.X., Wang, Q., 2013b. A 16-kyr lake level record inferred
398 from macrofossils in a sediment core from Genggahai Lake, northeastern Qinghai-Tibetan Plateau
399 (China). *J. Paleolimn.* 49, 575–590.

400 Qiang, M.R., Song, L., Jin, Y. X., Li, Y., Liu, L., Zhang, J.W., Zhao, Y., Chen, F.H., 2017. A 16-kyroxygen-
401 isotope record from Genggahai Lake on the northeastern Qinghai-Tibetan Plateau: hydroclimatic
402 evolution and changes in atmospheric circulation. *Quat. Sci. Rev.* 162, 72–87.

403 Reimer, P.J., Baillie, M.G.L., Bard, E., Bayliss, A., Beck, J.W., Bertrand, C.J.H., Blackwell, P.G., Buck, C.E.,
404 Burr, G.S., Culter, K.B., Damon, P.E., Edwards, R.L., Fairbanks, R.G., Friedrich, M., Guilderson, T.P.,
405 Hogg, A.G., Hughen, K.A., Kromer, B., McCormac, G., Manning, S., Ramsey, C.B., Reimer, R.W.,
406 Remmele, S., Southon, J.R., Stuiver, M., Talamo, S., Taylor, F.W., van der Plicht, J., Weyhenmeyer, C.E.,
407 2009. IntCal09 and Marine09 radiocarbon age calibration curves, 0–50,000 years cal BP. *Radiocarbon* 51,
408 1111–1150.

409 Shen, J., Liu, X.Q., Wang, S.M., Matsumoto, R., 2005. Palaeoclimatic changes in the Qinghai Lake area
410 during the last 18,000 years. *Quat. Int.* 136, 131–140.

411 Walseng, B., 2016a. *Chydorus sphaericus* O.F.M. Artsdatabanken. Norwegian Institute of Environmental
412 Research. Available at <https://www.artsdatabanken.no/Pages/214507/>. Cited 27. September 2020.

413 Walseng, B., 2016b. *Alona rectangula* Sars. Artsdatabanken. Norwegian Institute of Environmental Research.
414 Available at <https://www.artsdatabanken.no/Pages/214487/>. Cited 27. September 2020.

415 Wang, Y.J., Cheng, H., Edwards, R.L., He, Y.Q., Kong, X.G., An, Z.S., Wu, J.Y., Kelly, M.J., Dykoski, C.A.,
416 Li, X.D., 2005. The Holocene Asian Monsoon: links to solar changes and North Atlantic Climate. *Science*
417 308, 854–857.

418 Webster, P.J., Magaña, V.O., Palmer, T.N., Shukla, J., Thomas, R.A., Yanai, M., Yasunari, T., 1998. Monsoons:
419 Processes, predictability, and the prospects for prediction. *J. Geophys. Res.-Atmos.* 103, 14451–14510.

420 Weckström, J., Korhola, A., Blom, T., 1997. The Relationship between Diatoms and Water Temperature in
421 Thirty Subarctic Fennoscandian Lakes. *Arct. Antarct. Alp. Res.* 29, 75–92.

422 Wei, H.C., E, C.Y., Zhang, J., Sun, Y.J., Li, Q.K., Hou, G.L., Duan, R.L., 2020. Climate change and
423 anthropogenic activities in qinghai lake basin over the last 8500 years derived from pollen and charcoal
424 records in an aeolian section. *Catena* 193, 104616.

425 Wen, R.L., Xiao, J.L., Chang, Z.G., Zhai, D.Y., Xu, Q.H., Li, Y.C., Itoh, S., Lomtatidze, Z., 2010. Holocene
426 climate changes in the mid-high-latitude-monsoon margin reflected by the pollen record from Hulun Lake,
427 northeastern Inner Mongolia. *Quat. Res.* 73, 293–303.

428 Wen, R.L., Xiao, J.L., Fan, J.W., Zhang, S.R., Yamagata, H., 2017. Pollen evidence for amid-Holocene East
429 Asian summer monsoon maximum in northern China. *Quat. Sci. Rev.* 176, 29–35.

430 Wilson, G.P., Reed, J.M., Frogley, M.R., Hughes, P.D., Tzedakis, P.C., 2015. Reconciling diverse lacustrine
431 and terrestrial system response to penultimate deglacial warming in southern Europe. *Geology* 43, 819–
432 822.

433 Wilson, L.R., 1941. The larger aquatic vegetation of Trout Lake, Vilas County, Wisconsin. *Transactions of the*
434 *Wisconsin Academy of Science Arts & Letters* 33, 135–146.

435 Xiao, J.L., Xu, Q.H., Nakamura, T., Yang, X.L., Liang, W.D., Inouchi, Y., 2004. Holocene vegetation
436 variation in the Daihai Lake region of north-central China: a direct indication of the Asian monsoon
437 climatic history. *Quat. Sci. Rev.* 23, 1669–1679

438 Zhang, M.M., Bu, Z.J., Wang, S.Z., Jiang, M., 2019. Moisture changes in Northeast China since the last
439 deglaciation: Spatiotemporal out-of-phase patterns and possible forcing mechanisms. *Earth-Sci. Rev.* 201,
440 102984.

441 Zhao, Y., Liu, Y.L., Guo, Z.T., Fang, K.Y., Li, Q., Cao, X.Y., 2017. Abrupt vegetation shifts caused by gradual
442 climate changes in central Asia during the Holocene. *Sci. China-Earth Sci.* 60, 1317–1327.

443 Zhou, T., Gong, D., Li, J., Li, B., 2009. Detecting and understanding the multi-decadal variability of the East
444 Asian summer monsoon recent progress and state of affairs. *Meteorol. Z.*, 18, 455–467.

445 **Figure and table captions**

446 **Fig. 1.** Location and modern environmental context of Genggahai Lake. (A) Overview map showing locations
447 of the paleoclimatic sites referenced in the text, and the dominant circulation systems of the westerlies and the
448 Asian monsoon. Genggahai Lake is indicated by a star. Lakes Qinghai (Shen et al., 2005), Kuhai (Mischke et
449 al., 2010), Dalianhai (Cheng et al., 2013), Gonghai (Chen et al., 2015), Chagan Nur (Li et al., 2020a), Dali
450 (Wen et al., 2017), Daihai (Xiao et al., 2004) and Hulun (Wen et al., 2010), Dabusu Lake (Li and Lv, 2001)
451 and Dongge Cave (Dykoski et al., 2005) are indicated by circles. The modern Asian summer monsoon limit is
452 shown by a green dashed line (after Gao et al., 1962). (B) Physical environment of the Gonghe Basin.
453 Mountain areas above 4,500 m a.s.l. and the potential catchment area of groundwater-fed Genggahai Lake are
454 delineated by the white dashed line and the blue dashed line (after Qiang et al., 2017), respectively. (C)
455 Vegetation (after Qiang et al., 2013b.) and coring sites.

456 **Fig. 2.** Records of plant macrofossils (A–F), Cladocera (G, H), and diatoms (I, J, K) from the sediments of
457 Genggahai Lake and the reconstructed lake level (L). (G, I, J) Relative abundance of Cladocera, planktonic
458 diatoms and non-planktonic diatoms, respectively. (H, K) Total counted individuals of Cladocera and diatoms,
459 respectively. In (A, C, E) green and red bars denote *Potamogeton pectinatus* (or *Myriophyllum spicatum*) and
460 *Chara* encrustations, respectively. Macrofossil stem encrustations are identified in the stratigraphy. *Chara*
461 gyrogonites are presented as individuals/dm² per year.

462 **Fig. 3.** Comparison of the synthesized tree pollen index (J, this study) and pollen records from the marginal
463 regions dominated by the ASM. (A, B) Total terrestrial pollen concentration from lakes Genggahai (this study)
464 and Qinghai (Shen et al., 2005), respectively. (C–I) Tree pollen percentages from lakes Genggahai (this study),
465 Qinghai (Shen et al., 2005), Dalianhai (Cheng et al., 2013), Gonghai (Chen et al., 2015), Dali (Wen et al.,
466 2017), Daihai (Xiao et al., 2004) and Hulun (Wen et al., 2010), respectively. The gray bar indicates the optimal
467 vegetation conditions during 8.6–6.9 cal kyr BP.

468 **Fig. 4.** Comparison of the lake-level record (A) and total terrestrial pollen concentration (I) from Genggahai
469 Lake and other paleoclimatic records. (B) Asian summer monsoon (ASM) index based on the sedimentary
470 carbonate and TOC content of the sediments of Qinghai Lake (An et al., 2012). (C) Simulated water level of
471 Qinghai Lake (Li et al., 2020b). (d) Mz (ϕ) grain-size record from Dabusu Lake (Li and Lv, 2001). (E, F)
472 Water level of Chagan Nur (Li et al., 2020a) and Dali Lake (Goldsmith et al., 2017), respectively. (G) Summer
473 insolation at 35°N (Berger and Loutre, 1991). (H) $\delta^{18}\text{O}_c$ record from Dongge Cave (Dykoski et al., 2005). (J)
474 Synthesized tree pollen index (this study). (K) Probability density plot of the OSL ages of eolian sand samples
475 from the NETP (Qiang et al., 2013a). (L) Synthesized sand percentages in eolian deposits in northeast China
476 (Li et al., 2014).

Lateglacial and Holocene climate change in the NE Tibetan Plateau: Reconciling divergent proxies of Asian summer monsoon variability

Yuan Li^{a, c}, Mingrui Qiang^{b, c*}, Xiaozhong Huang^c, Yongtao Zhao^a, Jaakko J. Leppänen^d, Jan Weckström^d, Minna Väliranta^d

^a Key Laboratory of Desert and Desertification, Northwest Institute of Eco-Environment and Resources, Chinese Academy of Sciences, Lanzhou 730000, China.

^b School of Geography, South China Normal University, Guangzhou 510631, China

^c Key Laboratory of Western China's Environmental Systems (MOE), College of Earth and Environmental Sciences, Lanzhou University, Lanzhou 730000, China.

^d Environmental Change Research Unit, Ecosystems and Environment Research Programme and Helsinki Institute of Sustainability Science, Faculty of Biological and Environmental Sciences, P.O. Box 65, 00014 University of Helsinki, Finland.

Corresponding author: Mingrui Qiang (mrqiang@scnu.edu.cn).

Abstract

The nature of Holocene Asian summer monsoon (ASM) evolution documented by diverse natural archives remains controversial, with a contentious issue being whether or not a strong Asian summer monsoon prevailed during the early Holocene. Here we present sequences of multiple proxies measured in sediment cores from Genggahai Lake in the NE Tibetan Plateau (NETP). The results suggest that a higher lake level and relatively lower terrestrial vegetation cover occurred synchronously during the early Holocene (11.3–8.6 kyr cal BP), compared with the period from 8.6 to 6.9 kyr cal BP. This finding clearly reflects the existence of different hydroclimatic conditions between the lake and its catchment due to diverse driving mechanisms. The early Holocene high stand of the lake, as demonstrated by the stratigraphic variability of the remains of aquatic biota, may have responded to the strengthened ASM and increased monsoonal precipitation; the relatively low vegetation cover in the marginal region of the Asian monsoon during the early Holocene, and the coeval widespread active sand dune mobility in both the NE Tibetan Plateau and NE China, most likely resulted from a low level of effective moisture due to high evaporation, and hence they cannot be interpreted as evidence of a weak ASM. Our results potentially reconcile the current divergent interpretations of various proxy climate records from the region. Our findings suggest that the ASM evolution was characterized by a consistent pattern across the monsoonal regions, as indicated by the oxygen isotope record of Chinese speleothems.

33 *Key words:* Holocene; monsoon; China; Micropaleontology; lake level; vegetation.

34 **1 Introduction**

35 The Asian monsoon system affects more than half of the world's population and the
36 associated ecosystems (Webster et al., 1998). Understanding the variability of the Asian
37 monsoon has significant implications for the social and ecological systems in the region (Hansen
38 and Lebedeff, 1987; Mishra et al., 2019). Precipitation in the marginal regions dominated by the
39 Asian summer monsoon (ASM) is highly dependent on the strength of the ASM: a stronger ASM
40 circulation can transport more water vapor, leading to higher precipitation, and vice versa (Zhou
41 et al., 2009). Therefore, precipitation in these marginal regions can directly reflect the strength of
42 the ASM (Chen et al., 2015). Over the past two decades, numerous studies of the Holocene
43 evolution of the ASM have been conducted based on diverse natural archives from the region
44 (e.g., Chen et al., 2015; Dykoski et al., 2005; Goldsmith et al., 2017; Hu et al., 2008; Li et al.,
45 2014; Wang et al., 2005; Wei et al., 2020). However, the nature of ASM evolution during the
46 Holocene still remains controversial, with a contentious issue being whether or not a strong
47 Asian summer monsoon prevailed during the early Holocene. For example, the early Holocene
48 high-stand of lakes in the marginal regions dominated by the ASM (Fig. 1A), including lakes
49 Dali (Goldsmith et al., 2017), Dabusu (Li and Lv, 2001) and Kuhai (Mischke et al., 2010),
50 reflects an intensified ASM which is consistent with monsoonal records from Chinese
51 speleothems (Dykoski et al., 2005; Hu et al., 2008; Wang et al., 2005). However, records of
52 pollen assemblages and/or pollen-based precipitation from the lakes in the region (Fig. 1A),
53 including lakes Gonghai (Chen et al., 2015), Dalianhai (Cheng et al., 2013), Daihai (Xiao et al.,
54 2004), Dali (Wen et al., 2017) and Hulun (Wen et al., 2010), together with evidence for
55 widespread sand dune mobility in NE China (Li et al., 2014), indicate the occurrence of dry
56 terrestrial conditions at this time, possibly related to a weak ASM. Furthermore, even diverse
57 proxies generated from the same study site may exhibit divergent patterns of Holocene climate
58 change and ASM evolution. For example, at Qinghai Lake, the geochemical proxies (An et al.,
59 2012; Jin et al., 2015; Lister et al., 1991) generally suggest a high lake level and a strong ASM
60 during the early Holocene. In contrast, the shoreline deposits (Liu et al., 2015) and the pollen
61 assemblages (Shen et al., 2005) suggest that the lake level probably was low at this time, induced
62 by high evaporation or a weak ASM. These seemingly contradictory interpretations, especially
63 those from the same site (e.g., Qinghai Lake), cannot be explained by the spatial and temporal
64 differentiation of ASM evolution, or by chronological uncertainties. Therefore, a comprehensive
65 analysis of the driving mechanisms of these proxies and their linkage to the ASM are essential
66 for reconciling the controversy.

67 Genggahai Lake is a small, shallow lake in the NE Tibetan Plateau (NETP) (Fig. 1A),
68 located in the marginal region dominated by the ASM. The sediments are rich in the remains of
69 aquatic biota and terrestrial pollen, which provide the opportunity to conduct multi-proxy
70 investigations of ASM evolution. Qiang et al. (2013b) have discussed the lake-level fluctuations
71 over the past 16 kyr based mainly on plant macrofossil assemblages in the sediments from a
72 single core (GGH-A) recovered from the lake. However, the early Holocene high-stand of the
73 lake was indirectly inferred by geochemical variables (total organic carbon, total nitrogen and
74 carbon isotopic composition of bulk sediment organic matter), due to the absence of plant
75 macrofossils (Qiang et al., 2013b). In addition, the evolution of lake bathymetry may also lead to
76 lake-level fluctuations on a long timescale (Hilton, 1985; Lehman, 1975), which was not
77 differentiated from the influence of climatic factors in the previous study (Qiang et al., 2013b).
78 Therefore, comprehensive analyses of diverse bioindicators (e.g., plant macrofossils, Cladocera,
79 diatoms) from multiple cores are essential not only for the reliable reconstruction of lake-level
80 fluctuations, but also for assessing the influence of the evolution of lake bathymetry on the lake-
81 level fluctuations, and for understanding regional hydroclimatic changes (Dearing, 1997).
82 Moreover, the evolution of the regional terrestrial vegetation and its potential linkages to the
83 ASM remain unclear.

84 Here we present sequences of aquatic (plant macrofossils, Cladocera, diatoms) and
85 terrestrial (terrestrial pollen) proxies derived from multiple sediment cores from Genggahai
86 Lake. Combined with hydrological and ecological investigations of the modern lake, and with
87 reference to independent climatic records from the marginal regions dominated by the ASM, our
88 aims were to reconstruct the regional ASM variability during the Lateglacial and the Holocene,
89 and to reconcile the current divergent results of proxy indicators of ASM evolution.

90 **2 Materials and Methods**

91 Genggahai Lake (36°11'N, 100°06'E) is located in the central Gonghe Basin (Fig. 1B) at
92 an altitude of 2,860 m a.s.l. The lake is small (surface area, ~2 km²) and shallow (maximum
93 water depth, ~1.8 m) and has an elevated salinity (~1.2 g L⁻¹) and pH (~9.1). *Potamogeton*
94 *pectinatus*, *Myriophyllum spicatum*, and *Chara* spp. dominate the submerged macrophyte
95 communities in the current lake. The lake is mainly fed by groundwater. Several small spring-
96 water streams flow into the lake. Three sediment cores were recovered from Genggahai Lake in
97 January 2008 and January 2013 using a modified Livingstone piston corer. Cores GGH-A (length
98 782 cm) and GGH-C (length 774 cm) were recovered from the center of the lake in a water depth
99 of 170 cm (Fig. 1C), and core GGH-E (length 765 cm) was recovered from the northwest littoral
100 area in a water depth of 110 cm (Fig. 1C). Due to the lack of terrestrial plant remains, samples of

101 the leaves of aquatic macrophytes were picked from the sediments for accelerator mass
102 spectrometry (AMS) ^{14}C dating, conducted by Beta Analytic Inc. (Miami, USA) (Table S1). The
103 reservoir age of the lake was estimated at 1,010 ^{14}C years on average, based on the AMS ^{14}C
104 dating results of the dissolved inorganic carbon of the lake water, macrophyte remains in the
105 lake's surface sediments and living *P. pectinatus* (Li et al., 2017b). A total of 26 ^{14}C ages from
106 cores GGH-A (cited from Qiang et al. 2013b), GGH-C, and GGH-E (Table S1), which are in
107 stratigraphic order, were calibrated to calendar years (Calib 6.0.1, Reimer et al., 2009) after
108 subtracting an average reservoir age (1,010 yr). The age-depth models of the three cores were
109 generated by the Bacon Bayesian age-modeling software (Blaauw and Christen, 2011), using the
110 calibrated radiocarbon ages. The age versus depth profiles of the three cores agree well with each
111 other, which supports their reliability (Fig. S1).

112 Plant macrofossils, including *Chara* gyrogonites (Fig. 2B, 2D, 2F) and encrustations of
113 *Chara* spp. and *P. pectinatus* (or *M. spicatum*) (Fig. 2A, 2C, 2E), were picked from cores GGH-
114 A (cited from Qiang et al. 2013b), GGH-C, and GGH-E. Cladocera (Fig. 2G) and diatom (Fig. 2I,
115 2G) analyses were conducted on core GGH-C using standard methods (Korhola and Rautio,
116 2001; Weckström et al., 1997). In addition, fossil pollen (Fig. 3A, 3C) was extracted from core
117 GGH-A following the methods of Fægri and Iversen (1989). In order to comprehensively depict
118 the terrestrial vegetation conditions in the marginal regions dominated by the ASM, we compiled
119 six lacustrine tree pollen records from the region, including from lakes Qinghai (Shen et al.,
120 2005), Dalianhai (Cheng et al., 2013), Gonghai (Chen et al., 2015), Dali (Wen et al., 2017),
121 Daihai (Xiao et al., 2004) and Hulun (Wen et al., 2010). Since the changes in the tree pollen
122 content of these records show a similar trend, a synthesized tree pollen index covering the past
123 12 kyr (obtained by taking the average of the normalized tree pollen contents from the six lakes)
124 was used to portray changes in tree cover in the marginal regions dominated by the ASM
125 (Fig. 3). Further details about the method are given in the supplements.

126 **3 Results and discussion**

127 3.1. Patterns of hydroclimatic evolution indicated by lake level and pollen sequences

128 In general, submerged macrophytes, Cladocera, and diatoms in freshwater lakes are
129 sensitive to changes in water level, and thus their fossil remains in lake sediments can be used to
130 reconstruct past water-level fluctuations (Birks, 1993; Heggen et al., 2012). The aquatic plant
131 macrofossils in the sediments of Genggahai Lake mainly originate from *Chara* spp.,
132 *P. pectinatus* and *M. spicatum*. These species also dominate the lake today and they are common
133 in shallow lakes worldwide (Wilson et al., 1941). The spatial distribution of submerged
134 macrophytes in the modern lake is mainly modulated by the water depth, and the shallow water

135 zone of the lake is occupied by *Chara* spp. (Fig. S2) (Qiang et al., 2013b). Therefore, the
136 occurrence of the fossil remains of *Chara* spp. and *P. pectinatus* (or *M. spicatum*) in the lake
137 sediments, especially the occurrence of abundant *Chara* gyrogonites, most likely reflects a
138 shallow water environment. As for fossil Cladocera, only two littoral species (*Chydorus*
139 *sphaericus* and *Coronatella rectangula*) which prefer macrophyte habitats were identified in the
140 sediments of Lake Genggahai (Walseng, B., 2016a, 2016b). Diatoms in the sediments are
141 relatively diverse, consisting of both planktonic (e.g., *Lindavia comta* and *Cyclotella*
142 *distinguenda*) and non-planktonic species (e.g., *Gomphonema angustum* and *Achnanthes*
143 *minutissima*). Based on changes in submerged macrophytes, Cladocera and diatoms in the lake
144 sediments (Fig. 2), the history of lake-level fluctuations was divided into the following four
145 stages:

146 **15.4–11.3 cal kyr BP** The lake sediments contain abundant submerged-macrophyte
147 encrustations, *Chara* gyrogonites and littoral cladoceran fossils, reflecting a shallow lake. In
148 addition, the diatom assemblages are dominated by both planktonic (e.g., *L. comta* and *C.*
149 *distinguenda*) and non-planktonic species (e.g., *G. angustum*). Notably, *C. distinguenda* is a
150 *tychoplanktonic species* which can adapt to shallow water conditions. Therefore, the lake level
151 most likely was low during this period.

152 **11.3–8.6 cal kyr BP** Submerged macrophytes and Cladocera largely disappear from the
153 sediments. In addition, the diatom assemblages are dominated by an euplanktonic species (i.e., *L.*
154 *comta*). Thus we conclude that the lake level was high during this period, and it may have
155 exceeded the depth limit for submerged macrophytes, resulting in the absence of Cladocera
156 macrophyte habitats and increasing the abundance of planktonic diatoms.

157 **8.6–5.5 cal kyr BP** Submerged macrophyte encrustations occur episodically and *Chara*
158 gyrogonites are relatively scarce. Cladocera fossils largely disappear from the sediments,
159 probably in response to the scarcity of macrophyte habitats. The diatom assemblages are
160 dominated by both planktonic (e.g., *L. comta* and *C. distinguenda*) and non-planktonic species.
161 Thus we conclude that the lake level during this period was probably high overall, but lower than
162 during the previous stage.

163 **5.5 kyr cal BP to the present** The lake sediments contain abundant submerged-
164 macrophyte encrustations, *Chara* gyrogonites, littoral Cladocera fossils, and non-planktonic
165 diatoms, reflecting a shallow lake.

166 The terrestrial pollen in lake sediments is mainly derived from the catchment and hence it
167 reflects the local and regional terrestrial vegetation conditions (Pennington, 1979). Changes in
168 total terrestrial pollen concentrations (Fig. 3A) and tree pollen contents (Fig. 3C) in the

169 sediments of Genggahai Lake are largely in agreement with those at nearby Qinghai Lake (Fig.
170 3B, 3D) and the synthesized tree pollen index (Fig. 3J), showing that optimal vegetation
171 conditions occurred during 8.6–6.9 cal kyr BP. Overall, the aquatic and animal fossils
172 (macrophytes, Cladocera, diatoms) and terrestrial pollen in the sediments of Genggahai Lake
173 indicate that a higher lake level and relatively lower terrestrial vegetation cover occurred
174 synchronously during the early Holocene (11.3–8.6 kyr cal BP), compared with the period from
175 8.6 to 6.9 kyr cal BP. This implies the occurrence of different hydroclimatic conditions between
176 the lake and its catchment (Fig. 4A, 4I). This apparent contradiction is also reflected in proxy
177 sequences from other lakes in the marginal regions dominated by the ASM: e.g., at Lakes
178 Qinghai (An et al., 2012; Shen et al., 2005), Dali (Goldsmith et al., 2017; Wen et al., 2017) and
179 Chagan Nur (Li et al., 2020a).

180 3.2. Implications for the evolution of the Asian summer monsoon

181 The early Holocene high lake levels and low total pollen concentrations (or tree
182 percentages) recorded by lake sediments from the margins of the regions dominated by the ASM
183 are mutually contradictory in terms of their interpretation as evidence for ASM strength (e.g., An
184 et al., 2012; Chen et al., 2015), or as evidence for the spatial differentiation of ASM evolution
185 (Zhang et al., 2019). However, these seemingly contradictory patterns most likely reflect the
186 existence of different hydroclimatic conditions between the lake and its catchment due to diverse
187 driving mechanisms (cf., Wilson et al., 2015), and they cannot simultaneously be interpreted as
188 proxies of ASM strength.

189 In general, lake-level fluctuations are controlled by the water balance of the lake.
190 However, previous studies have demonstrated that the evolution of lake bathymetry on a long
191 timescale may also result in lake-level fluctuations (Hilton, 1985; Lehman, 1975). Increased
192 allochthonous input of detrital materials will enhance the sedimentation rate in the deepest parts
193 of the lake due to gravity (i.e., the “sediment-focusing effect”) which will lead to decreases in
194 water depth (Hilton, 1985). However, at Genggahai Lake, the AMS ¹⁴C dating results show that
195 the sedimentation rate of the central cores (GGH-A and GGH-C) was largely consistent with that
196 of the littoral core (GGH-E) during the Lateglacial and Holocene (Fig. S1), indicating that
197 changes in lake bathymetry since the Lateglacial were probably minor, exerting little effect on
198 the lake level. This could be ascribed to the flat lake basin morphometry and the dense growth of
199 submerged macrophytes, which largely restricted re-suspension and transport of sediments to the
200 depocenter (cf. Dearing, 1997). Therefore, lake-level fluctuations mainly represent the balance
201 between water inflows and losses. Currently, there are no large glaciers on the summits of the
202 mountains surrounding Genggahai Lake. In addition, the Lateglacial glaciers on these mountains

203 were mainly distributed in areas above 4,500 m a.s.l. (Fig. 1B) (Li et al., 1991) and therefore
204 their total extent was relatively small. Thus they are unlikely to have continuously contributed
205 meltwater which could sustain the high lake level during the early Holocene (11.3–8.6 kyr
206 BP), given the temperature increase of ~3 °C at the onset of the Holocene (Herzschuh et al., 2014;
207 Li et al., 2017a). Genggahai Lake is fed mainly by groundwater. Loose, porous fluvio-lacustrine
208 sediments of the Gonghe Formation (Perrineau et al., 2011) and surficial fluvial-fan sediments
209 largely constitute the catchment substrate of groundwater. In addition, the deep incision of the
210 Yellow River in the eastern Gonghe Basin led to a steep hydraulic gradient of the basin
211 (Craddock et al., 2010). Therefore, the catchment of groundwater was highly permeable, and
212 hence precipitation can infiltrate rapidly into the ground and feed the lake. The evaporation
213 losses during the infiltration process were most likely low. In addition, the catchment area of the
214 groundwater feeding the lake is far larger than the lake's surface area (Fig. 1B). Therefore,
215 evaporation may play a minor role in the water balance of the lake, and hence the lake-level
216 fluctuations can be interpreted as indicating changes in regional precipitation, reflecting the
217 strength of the ASM in the study area. The pattern of water-level fluctuations at Genggahai Lake
218 largely coincides with that of other lakes in the marginal regions dominated by the ASM (e.g.,
219 Qinghai, Kuhai, Dali, Dabusu and Chagan Nur) (Fig. 4B–F). This consistent pattern suggests a
220 weak ASM during 15.4–11.3 cal kyr BP, a significantly intensified ASM during 11.3–8.6 cal
221 kyr BP, and a gradually weakening ASM thereafter. In addition, the results of a modeling study
222 of water level changes at Qinghai Lake also reveal an early Holocene high-stand (Fig. 4C) (Li et
223 al., 2020b).

224 The evolution of terrestrial vegetation is generally the integrated reactions to multiple
225 environmental factors, including temperature, precipitation and the available water capacity of
226 the soil (Prentice et al., 1992). The sparse terrestrial vegetation in the marginal regions
227 dominated by the ASM during 15.4–11.3 cal kyr BP and 5.5–0 cal kyr BP mainly resulted from
228 low monsoonal precipitation and low temperatures (Lu et al., 2011). In addition, the relatively
229 low total terrestrial pollen concentration (Fig. 4I) during the early Holocene (11.3–8.6 kyr cal BP)
230 suggests that the terrestrial vegetation did not respond to the significantly ameliorated
231 environmental conditions, although the monsoonal precipitation increased sharply. Significantly,
232 changes in terrestrial vegetation are modulated mainly by effective moisture rather than by
233 precipitation (Prentice et al., 1992). Furthermore, changes in effective moisture do not always
234 respond linearly to variations in precipitation, but rather they depend on the balance between
235 precipitation and evaporation. Therefore, the relatively low terrestrial vegetation cover in the
236 study area during the early Holocene mostly likely reflects a low level of effective moisture.
237 Notably, the low effective moisture during this interval is also documented by the widespread

238 sand dune mobility in both the NETP and NE China (Fig. 4K, 4L) (Li et al., 2014; Qiang et al.,
239 2013a). Given that the enhanced monsoonal precipitation during the early Holocene may have
240 infiltrated rapidly into the ground due to the porous nature of the soils and the steep hydraulic
241 gradient of the catchment, the water retained in the soils probably could not compensate for the
242 intense evaporation loss as a consequence of the high temperatures (Li et al., 2017a) and high
243 summer insolation. This may have led to a low level of effective moisture and further restricted
244 the development of both the terrestrial vegetation and paleosols (Mason et al., 2009; Qiang et al.,
245 2013a, 2016). In addition, the strong ASM during this period would have resulted in the strong
246 release of latent heat by water (Herzschuh et al., 2014), which may have further increased
247 temperatures and evaporation. By contrast, decreased temperatures (Li et al., 2017a), due to the
248 reduction in both summer insolation and release of latent heat by water vapor during the period
249 from 8.6 to 6.9 cal kyr BP, likely resulted in the weakened evaporation of soil water and hence
250 led to the widespread development of vegetation (Fig. 3) and palaeosols (Li et al., 2014; Qiang et
251 al., 2013a) in the marginal regions dominated by the ASM. In addition, given that the terrestrial
252 vegetation has a lagged response to precipitation changes, the different response rates of the lake
253 water and terrestrial vegetation to climate change may also have contributed to the occurrence of
254 different hydroclimatic conditions between Genggahai Lake and its catchment (Zhao et al.,
255 2017).

256 The diverse proxies derived from sediments of Genggahai Lake clearly reveal the
257 synchronous occurrence of high lake levels and relatively low terrestrial vegetation cover, which
258 are correlative with evidence for widespread sand dune mobility in the marginal regions
259 dominated by the ASM during the early Holocene. These features do not reflect different
260 climatic patterns, but rather they reflect different aspects of monsoonal climate change. The
261 consistent high-stand of the lakes from these monsoon margin areas suggests increased
262 monsoonal precipitation during the early Holocene, providing compelling evidences for the
263 spatial consistency of ASM evolution documented by oxygen isotopic records from Chinese cave
264 deposits (Cheng et al., 2019; Dykoski et al., 2005; Hu et al., 2008; Wang et al., 2005). The strong
265 ASM and the increased monsoonal precipitation in the marginal regions dominated by the ASM
266 during the early Holocene are ascribed to the enhanced thermal contrast between land and sea in
267 spring and summer due to the increased orbitally-induced summer insolation (Fig. 4G, 4H). The
268 relatively low terrestrial vegetation cover during the early Holocene, as well as the widespread
269 dune sands in eolian sections in both the NETP and NE China, most likely reflect low effective
270 moisture conditions due to high evaporation, and hence they cannot be interpreted as evidence of
271 a weak monsoon.

272 **4 Conclusions**

273 The water-level fluctuations of Genggahai Lake and the vegetation conditions in its
274 catchment were reconstructed from the aquatic biota and pollen preserved in the lake sediments.
275 The results suggest a higher lake level and a stronger ASM during 11.3–5.5 cal kyr BP,
276 compared to the intervals of 15.4–11.3 cal kyr BP and 5.5–0 cal kyr BP. However, the total
277 terrestrial pollen concentration indicates relatively lower terrestrial vegetation cover during the
278 early Holocene (11.3–8.6 cal kyr BP), compared with the period from 8.6 to 6.9 kyr cal BP. In
279 contrast to the lake-level fluctuations, the vegetation cover in the catchment cannot be used as a
280 proxy for variations in monsoonal precipitation and thus ASM strength. Rather, the relatively
281 low vegetation cover mainly reflects a low level of effective moisture conditions, as a result of
282 intense evaporation due to high temperatures during the early Holocene.

283 **Declaration of Competing Interest**

284 The authors declare that they have no known competing financial interests or personal
285 relationships that could have appeared to influence the work reported in this paper.

286 **Acknowledgments**

287 We thank Dr. J. Bloemendal for his helpful comments and language improvements. This
288 research was supported by the National Natural Science Foundation of China (grants 41901103,
289 41671190, 41271219 and 41807440), the National Key R&D Program of China (grant
290 2017YFA0603402), and the Foundation for Excellent Youth Scholars of the “Northwest Institute
291 of Eco-Environment and Resources”, CAS.

292 **References**

- 293 An, Z.S., Colman, S.M., Zhou, W.J., Li, X.Q., Brown, E.T., Timothy Jull, A.J., Cai, Y.J., Huang, Y.S., Lu,
294 X.F., Chang, H., Song, Y.G., Sun, Y.B., Xu, H., Liu, W.G., Jin, Z.D., Liu, X.D., Cheng, P., Liu, Y., Ai, L.,
295 Li, X.Z., Liu, X.J., Yan, L.B., Shi, Z.G., Wang, X.L., Wu, F., Qiang, X.K., Dong, J.B., Lu, F.Y., Xu,
296 X.W., 2012. Interplay between the Westerlies and Asian monsoon recorded in Lake Qinghai sediments
297 since 32 ka. *Sci. Rep.* 2, 619–625.
- 298 Berger, A., Loutre, M.F., 1991. Isolation values for the climate of the last 10 million years. *Quat. Sci. Rev.* 10,
299 297–317.
- 300 Birks, H.H., 1993. The importance of plant macrofossils in late glacial climatic reconstructions: an example
301 from western Norway. *Quat. Sci. Rev.* 12, 719–726.
- 302 Blaauw, M., Christen, J.A., 2011. Flexible paleoclimate age depth models using an autoregressive gamma
303 process. *Bayesian Anal.* 6, 457–474.

304 Chen, F.H., Xu, Q.H., Chen, J.H., Birks, H.J., Liu, J.B., Zhang, S.R., Jin, L., An, C.B., Telford, R.J., Cao, X.Y.,
305 Wang, Z.L., Zhang, X.J., Selvaraj, K., Lu, H.Y., Li, Y.C., Zheng, Z., Wang, H.P., Zhou, A.F., Dong, G.H.,
306 Zhang, J.W., Huang, X.Z., Bloemendal, J., Rao, Z.G., 2015. East Asian summer monsoon precipitation
307 variability since the last deglaciation. *Sci. Rep.* 5, 11186.

308 Cheng, B., Chen, F.H., Zhang, J.W., 2013. Palaeovegetational and palaeoenvironmental changes since the last
309 deglacial in Gonghe Basin, northeast Tibetan Plateau. *J. Geogr. Sci.* 23, 136–146.

310 Cheng, H., Zhang, H.W., Zhao, J.Y., Li, H.Y., Ning, Y.F., Kathayat, G., 2019. Chinese stalagmite
311 paleoclimate researches: A review and perspective. *Sci. China-Earth Sci.* 62, 1489–1513.

312 Craddock, W.H., Kirby, E., Harkins, N.W., Zhang, H.P., Shi, X.H., Liu, J.H., 2010. Rapid fluvial incision
313 along the Yellow River during headwater basin integration. *Nat. Geosci.* 3, 209–213.

314 Dearing, J.A., 1997. Sedimentary indicators of lake-level changes in the humid temperate zone: a critical
315 review. *J. Paleolimn.* 18, 1–14.

316 Dykoski, C.A., Edwards, R.L., Cheng, H., Yuan, D.X., Cai, Y.J., Zhang, M.L., Lin, Y.S., Qing, J.M., An, Z.S.,
317 Revenaugh, J., 2005. A high-resolution, absolute-dated Holocene and deglacial Asian monsoon record
318 from Dongge Cave, China. *Earth Planet. Sci. Lett.* 233, 71–86.

319 Fægri, K., Iversen, J., 1989. *Textbook of Pollen Analysis*, fourth ed. John Wiley & Sons, Chichester.

320 Gao, Y.X., Xu, S.Y., Guo, Q.Y., Zhang, M.L., 1962. Monsoon regions in China and regional climates. In: Gao,
321 Y.X. (Ed.), *Some Problems on East-Asia Monsoon*. Science Press, Beijing, pp. 49–63 (in Chinese).

322 Goldsmith, Y., Broecker, W.S., Xu, H., Polissar, P.J., deMenocal, P.B., Porat, N., Lan, J.H., Cheng, P., Zhou,
323 W.J., An, Z.S., 2017. Northward extent of East Asian monsoon covaries with intensity on orbital and
324 millennial timescales. *Proc. Natl. Acad. Sci.* 114, 1817–1821.

325 Hansen, J., Lebedeff, S., 1987. Global trends of measured surface air temperature. *J. Geophys. Res.-Atmos.* 92,
326 13345–13372.

327 Heggen, M.P., Birks, H.H., Heiri, O., Grytnes, J.A., Birks, H.J.B., 2012. Are fossil assemblages in a single
328 sediment core from a small lake representative of total deposition of mite, chironomid, and plant
329 macrofossil remains? *J. Paleolimn.* 48, 669–691.

330 Herzsuh, U., Borkowski, J., Schewe, J., Mischke, S., Tian, F., 2014. Moisture advection feedback supports
331 strong early-to-mid Holocene monsoon climate on the eastern Tibetan Plateau as inferred from a pollen-
332 based reconstruction. *Paleogeogr. Paleoclimatol. Paleoecol.* 402, 44–54.

333 Hilton, J.A., 1985. Conceptual framework for predicting the occurrence of sediment focusing and sediment
334 redistribution in small Lakes. *Limnol. Oceanogr.* 30, 1131–1143.

335 Hu, C.Y., Henderson, G.M., Huang, J.H., Xie, S.C., Sun, Y., Johnson, K.R., 2008. Quantification of Holocene
336 Asian monsoon rainfall from spatially separated cave records. *Earth Planet. Sci. Lett.* 266, 221–232.

337 Jin, Z.D., An, Z.S., Yu, J.M., Li, F.C., Zhang, F., 2015. Lake Qinghai sediment geochemistry linked to
338 hydroclimate variability since the last glacial. *Quat. Sci. Rev.* 122, 63–73.

- 339 Korhola, A., Rautio, M., 2001. Cladocera and other Branchiopod crustaceans. In: Smol, J.P., Birks, J.B., Last,
340 W.M. (Eds.), Tracking environmental change using lake sediments. Zoological indicators. Kluwer,
341 Dordrecht. pp. 5–41.
- 342 Lehman, J.T., 1975. Reconstructing the rate of accumulation of lake sediment: The effect of sediment focusing.
343 *Quat. Res.* 5, 541–550.
- 344 Li, G.Q., Wang, Z., Zhao, W.W., Jin, M., Wang, X.Y., Tao, S.X., Chen, C.Z., Cao, X.Y., Zhang, Y.N., Yang,
345 H., Madsen, D., 2020a. Quantitative precipitation reconstructions from Chagan Nur revealed lag response
346 of East Asian summer monsoon precipitation to summer insolation during the Holocene in arid northern
347 China. *Quat. Sci. Rev.* 239, 106365.
- 348 Li, J.J., Zhou, S.Z., Pan, B.T., 1991. The problems of Quaternary glaciation in the eastern part of Qinghai-
349 Xizang Plateau. *Quaternary Sciences* 3, 193–203 (in Chinese with English abstract).
- 350 Li, Q., Wu, H.B., Yu, Y.Y., Sun, A.Z., Markovic, S.B., Guo, Z.T., 2014. Reconstructed moisture evolution of
351 the deserts in northern China since the Last Glacial Maximum and its implications for the East Asian
352 summer monsoon. *Glob. Planet. Change* 121, 101–112.
- 353 Li, X.M., Wang, M.D., Zhang, Y.Z., Lei, L., Hou, J.Z., 2017a. Holocene climatic and environmental change
354 on the western Tibetan Plateau revealed by glycerol dialkyl glycerol tetraethers and leaf wax deuterium-
355 to-hydrogen ratios at Aweng Co. *Quat. Res.* 87, 455–467.
- 356 Li, Y., Qiang, M.R., Jin, Y.X., Liu, L., Zhou, A.F., Zhang, J.W., 2017b. Influence of aquatic plant
357 photosynthesis on the reservoir effect of Genggahai Lake, northeastern Qinghai-Tibetan Plateau.
358 *Radiocarbon* 60, 561–569.
- 359 Li, Y., Zhang, Y.X., Zhang, X.Z., Ye, W.T., Xu, L.M., Han, Q., Li, Y.C., Liu, H.B., Peng, S.M., 2020b. A
360 continuous simulation of Holocene effective moisture change represented by variability of virtual lake
361 level in East and Central Asia. *Sci. China-Earth Sci.* 63, 1161–1175.
- 362 Li, Z.F., Lv, J.F., 2001. Geomorphology, deposition and lake evolution of Dabusu Lake, Northeastern China.
363 *Journal of Lake Science*, 13, 103–110 (in Chinese).
- 364 Lister, G.S., Kelts, K.R., Chen, K.Z., Yu, J.Q., Niessen, F., 1991. Lake Qinghai, China: closed- basin lake
365 levels and the oxygen isotope record for ostracoda since the latest Pleistocene. *Paleogeogr. Paleoclimatol.*
366 *Paleoecol.* 84, 141–162.
- 367 Liu, X.J., Lai, Z.P., Madsen, D.B., Zeng, F.M., 2015. Last deglacial and Holocene lake level variations of
368 Qinghai Lake. *J. Quat. Sci.* 30, 245–257.
- 369 Lu, H.Y., Wu, N.Q., Liu, K.B., Zhu, L.P., Yang, X.D., Yao, T.D., Wang, L., Li, Q., Liu, X.Q., Shen, C.M., Li,
370 X.Q., Tong, G.B., Jiang, H., 2011. Modern pollen distributions in Qinghai-Tibetan Plateau and the
371 development of transfer functions for reconstructing Holocene environmental changes. *Quat. Sci. Rev.* 30,
372 947–966.
- 373 Mason, J.A., Lu, H., Zhou, Y., Miao, X., Swinehart, J.B., Liu, Z., Goble, R.J., Yi, S., 2009. Dune mobility and
374 aridity at the desert margin of northern China at a time of peak monsoon strength. *Geology* 37, 947–950.

375 Mischke, S., Zhang, C.J., Borner A, Herzsuh, U., 2010. Lateglacial and Holocene variation in aeolian
376 sediment flux over the northeastern Tibetan Plateau recorded by laminated sediments of a saline
377 meromictic lake. *J. Quat. Sci.* 25, 162–177.

378 Mishra, P.K., Ankit, Y., Gautam, P.K., Lakshmidivi, C.G., Singh, P., Anoop, A., 2019. Inverse relationship
379 between south-west and north-east monsoon during the late Holocene: Geochemical and sedimentological
380 record from Ennamangalam Lake, southern India. *Catena* 182, 104117.

381 Paillard, D., Labeyrie, L., Yiou, P., 1996. Macintosh program performs time-series analysis. *Eos, Transactions*
382 *American Geophysical Union*, 77, 379.

383 Pennington, W., 1979. The origin of pollen in lake sediments: an enclosed lake compared with one receiving
384 inflow streams. *New Phytol.* 83, 189–213.

385 Perrineau, A., van Der Woerd, J., Gaudemer, Y., Jing, L.-Z., Pik, R., Tapponnier, P., Thuizat, R., Zhang, Z.R.,
386 2011. Incision rate of the Yellow River in Northeastern Tibet constrained by ¹⁰Be and ²⁶Al cosmogenic
387 isotope dating of fluvial terraces: implications for catchment evolution and plateau building. *Geological*
388 *Society London Special Publication* 353, 189–219.

389 Prentice, I.C., Cramer, W., Harrison, S.P., Leemans, R., Monserud, R.A., Solomon, A.M., 1992. Special paper:
390 a global biome model based on plant physiology and dominance, soil properties and climate. *J. Biogeogr.*
391 117–134.

392 Qiang, M.R., Chen, F.H., Song, L., Liu, X.X., Li, M.Z., Wang, Q., 2013a. Late Quaternary aeolian activity in
393 Gonghe Basin, northeastern Qinghai-Tibetan plateau, China. *Quat. Res.* 79, 403–412.

394 Qiang, M.R., Jin, Y.X., Liu, X.X., Song, L., Li, H., Li, F.S., Chen, F.H., 2016. Late Pleistocene and Holocene
395 aeolian sedimentation in Gonghe Basin, northeastern Qinghai-Tibetan plateau: variability, processes, and
396 climatic implications. *Quat. Sci. Rev.* 132, 57–73.

397 Qiang, M.R., Song, L., Chen, F.H., Li, M.Z., Liu, X.X., Wang, Q., 2013b. A 16-kyr lake level record inferred
398 from macrofossils in a sediment core from Genggahai Lake, northeastern Qinghai-Tibetan Plateau
399 (China). *J. Paleolimn.* 49, 575–590.

400 Qiang, M.R., Song, L., Jin, Y. X., Li, Y., Liu, L., Zhang, J.W., Zhao, Y., Chen, F.H., 2017. A 16-kyroxygen-
401 isotope record from Genggahai Lake on the northeastern Qinghai-Tibetan Plateau: hydroclimatic
402 evolution and changes in atmospheric circulation. *Quat. Sci. Rev.* 162, 72–87.

403 Reimer, P.J., Baillie, M.G.L., Bard, E., Bayliss, A., Beck, J.W., Bertrand, C.J.H., Blackwell, P.G., Buck, C.E.,
404 Burr, G.S., Culter, K.B., Damon, P.E., Edwards, R.L., Fairbanks, R.G., Friedrich, M., Guilderson, T.P.,
405 Hogg, A.G., Hughen, K.A., Kromer, B., McCormac, G., Manning, S., Ramsey, C.B., Reimer, R.W.,
406 Remmele, S., Southon, J.R., Stuiver, M., Talamo, S., Taylor, F.W., van der Plicht, J., Weyhenmeyer, C.E.,
407 2009. IntCal09 and Marine09 radiocarbon age calibration curves, 0–50,000 years cal BP. *Radiocarbon* 51,
408 1111–1150.

409 Shen, J., Liu, X.Q., Wang, S.M., Matsumoto, R., 2005. Palaeoclimatic changes in the Qinghai Lake area
410 during the last 18,000 years. *Quat. Int.* 136, 131–140.

411 Walseng, B., 2016a. *Chydorus sphaericus* O.F.M. Artsdatabanken. Norwegian Institute of Environmental
412 Research. Available at <https://www.artsdatabanken.no/Pages/214507/>. Cited 27. September 2020.

413 Walseng, B., 2016b. *Alona rectangula* Sars. Artsdatabanken. Norwegian Institute of Environmental Research.
414 Available at <https://www.artsdatabanken.no/Pages/214487/>. Cited 27. September 2020.

415 Wang, Y.J., Cheng, H., Edwards, R.L., He, Y.Q., Kong, X.G., An, Z.S., Wu, J.Y., Kelly, M.J., Dykoski, C.A.,
416 Li, X.D., 2005. The Holocene Asian Monsoon: links to solar changes and North Atlantic Climate. *Science*
417 308, 854–857.

418 Webster, P.J., Magaña, V.O., Palmer, T.N., Shukla, J., Thomas, R.A., Yanai, M., Yasunari, T., 1998. Monsoons:
419 Processes, predictability, and the prospects for prediction. *J. Geophys. Res.-Atmos.* 103, 14451–14510.

420 Weckström, J., Korhola, A., Blom, T., 1997. The Relationship between Diatoms and Water Temperature in
421 Thirty Subarctic Fennoscandian Lakes. *Arct. Antarct. Alp. Res.* 29, 75–92.

422 Wei, H.C., E, C.Y., Zhang, J., Sun, Y.J., Li, Q.K., Hou, G.L., Duan, R.L., 2020. Climate change and
423 anthropogenic activities in qinghai lake basin over the last 8500 years derived from pollen and charcoal
424 records in an aeolian section. *Catena* 193, 104616.

425 Wen, R.L., Xiao, J.L., Chang, Z.G., Zhai, D.Y., Xu, Q.H., Li, Y.C., Itoh, S., Lomtatidze, Z., 2010. Holocene
426 climate changes in the mid-high-latitude-monsoon margin reflected by the pollen record from Hulun Lake,
427 northeastern Inner Mongolia. *Quat. Res.* 73, 293–303.

428 Wen, R.L., Xiao, J.L., Fan, J.W., Zhang, S.R., Yamagata, H., 2017. Pollen evidence for amid-Holocene East
429 Asian summer monsoon maximum in northern China. *Quat. Sci. Rev.* 176, 29–35.

430 Wilson, G.P., Reed, J.M., Frogley, M.R., Hughes, P.D., Tzedakis, P.C., 2015. Reconciling diverse lacustrine
431 and terrestrial system response to penultimate deglacial warming in southern Europe. *Geology* 43, 819–
432 822.

433 Wilson, L.R., 1941. The larger aquatic vegetation of Trout Lake, Vilas County, Wisconsin. *Transactions of the*
434 *Wisconsin Academy of Science Arts & Letters* 33, 135–146.

435 Xiao, J.L., Xu, Q.H., Nakamura, T., Yang, X.L., Liang, W.D., Inouchi, Y., 2004. Holocene vegetation
436 variation in the Daihai Lake region of north-central China: a direct indication of the Asian monsoon
437 climatic history. *Quat. Sci. Rev.* 23, 1669–1679

438 Zhang, M.M., Bu, Z.J., Wang, S.Z., Jiang, M., 2019. Moisture changes in Northeast China since the last
439 deglaciation: Spatiotemporal out-of-phase patterns and possible forcing mechanisms. *Earth-Sci. Rev.* 201,
440 102984.

441 Zhao, Y., Liu, Y.L., Guo, Z.T., Fang, K.Y., Li, Q., Cao, X.Y., 2017. Abrupt vegetation shifts caused by gradual
442 climate changes in central Asia during the Holocene. *Sci. China-Earth Sci.* 60, 1317–1327.

443 Zhou, T., Gong, D., Li, J., Li, B., 2009. Detecting and understanding the multi-decadal variability of the East
444 Asian summer monsoon recent progress and state of affairs. *Meteorol. Z.*, 18, 455–467.

445 **Figure and table captions**

446 **Fig. 1.** Location and modern environmental context of Genggahai Lake. (A) Overview map showing locations
447 of the paleoclimatic sites referenced in the text, and the dominant circulation systems of the westerlies and the
448 Asian monsoon. Genggahai Lake is indicated by a star. Lakes Qinghai (Shen et al., 2005), Kuhai (Mischke et
449 al., 2010), Dalianhai (Cheng et al., 2013), Gonghai (Chen et al., 2015), Chagan Nur (Li et al., 2020a), Dali
450 (Wen et al., 2017), Daihai (Xiao et al., 2004) and Hulun (Wen et al., 2010), Dabusu Lake (Li and Lv, 2001)
451 and Dongge Cave (Dykoski et al., 2005) are indicated by circles. The modern Asian summer monsoon limit is
452 shown by a green dashed line (after Gao et al., 1962). (B) Physical environment of the Gonghe Basin.
453 Mountain areas above 4,500 m a.s.l. and the potential catchment area of groundwater-fed Genggahai Lake are
454 delineated by the white dashed line and the blue dashed line (after Qiang et al., 2017), respectively. (C)
455 Vegetation (after Qiang et al., 2013b.) and coring sites.

456 **Fig. 2.** Records of plant macrofossils (A–F), Cladocera (G, H), and diatoms (I, J, K) from the sediments of
457 Genggahai Lake and the reconstructed lake level (L). (G, I, J) Relative abundance of Cladocera, planktonic
458 diatoms and non-planktonic diatoms, respectively. (H, K) Total counted individuals of Cladocera and diatoms,
459 respectively. In (A, C, E) green and red bars denote *Potamogeton pectinatus* (or *Myriophyllum spicatum*) and
460 *Chara* encrustations, respectively. Macrofossil stem encrustations are identified in the stratigraphy. *Chara*
461 gyrogonites are presented as individuals/dm² per year.

462 **Fig. 3.** Comparison of the synthesized tree pollen index (J, this study) and pollen records from the marginal
463 regions dominated by the ASM. (A, B) Total terrestrial pollen concentration from lakes Genggahai (this study)
464 and Qinghai (Shen et al., 2005), respectively. (C–I) Tree pollen percentages from lakes Genggahai (this study),
465 Qinghai (Shen et al., 2005), Dalianhai (Cheng et al., 2013), Gonghai (Chen et al., 2015), Dali (Wen et al.,
466 2017), Daihai (Xiao et al., 2004) and Hulun (Wen et al., 2010), respectively. The gray bar indicates the optimal
467 vegetation conditions during 8.6–6.9 cal kyr BP.

468 **Fig. 4.** Comparison of the lake-level record (A) and total terrestrial pollen concentration (I) from Genggahai
469 Lake and other paleoclimatic records. (B) Asian summer monsoon (ASM) index based on the sedimentary
470 carbonate and TOC content of the sediments of Qinghai Lake (An et al., 2012). (C) Simulated water level of
471 Qinghai Lake (Li et al., 2020b). (d) Mz (ϕ) grain-size record from Dabusu Lake (Li and Lv, 2001). (E, F)
472 Water level of Chagan Nur (Li et al., 2020a) and Dali Lake (Goldsmith et al., 2017), respectively. (G) Summer
473 insolation at 35°N (Berger and Loutre, 1991). (H) $\delta^{18}\text{O}_c$ record from Dongge Cave (Dykoski et al., 2005). (J)
474 Synthesized tree pollen index (this study). (K) Probability density plot of the OSL ages of eolian sand samples
475 from the NETP (Qiang et al., 2013a). (L) Synthesized sand percentages in eolian deposits in northeast China
476 (Li et al., 2014).

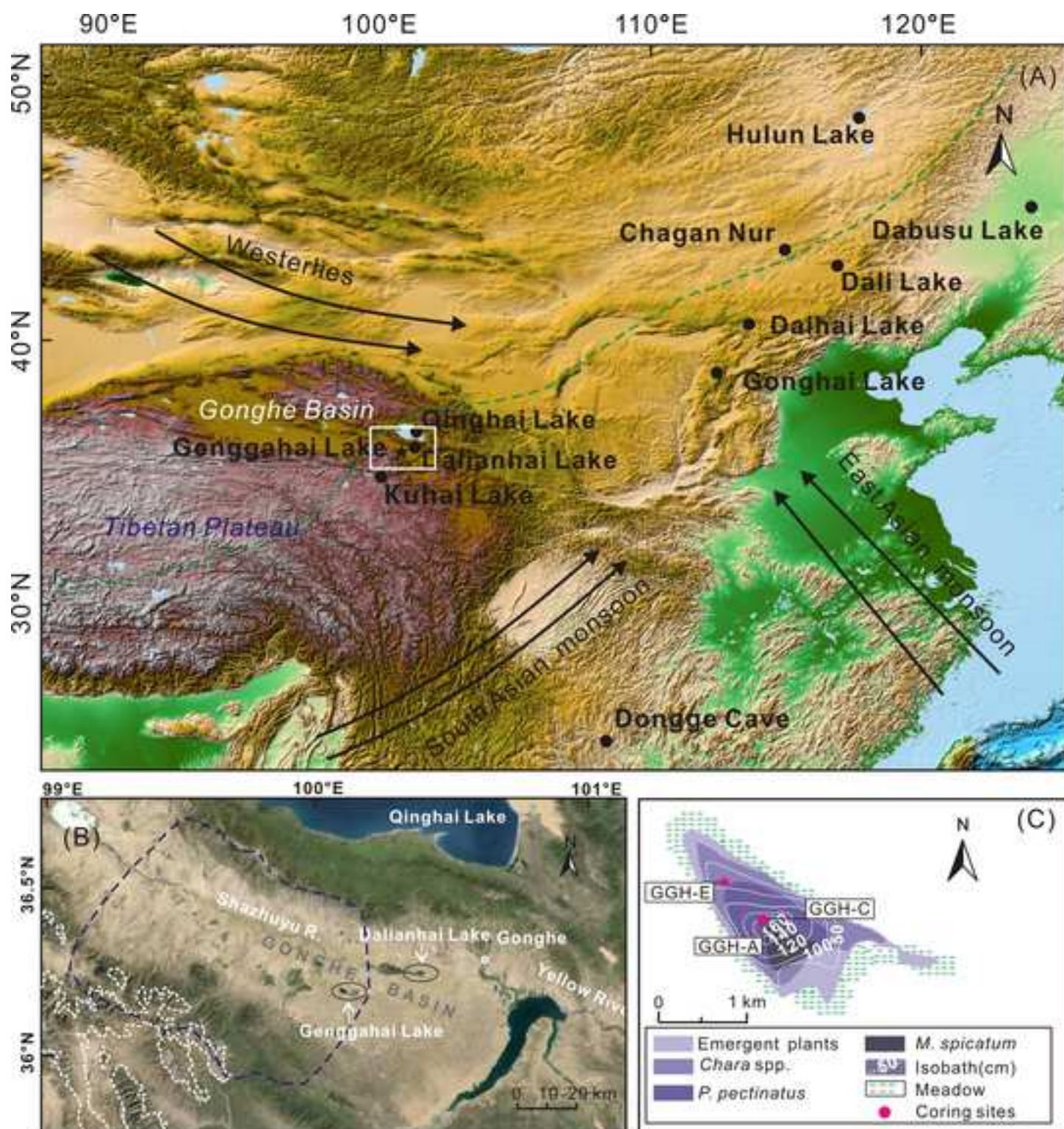
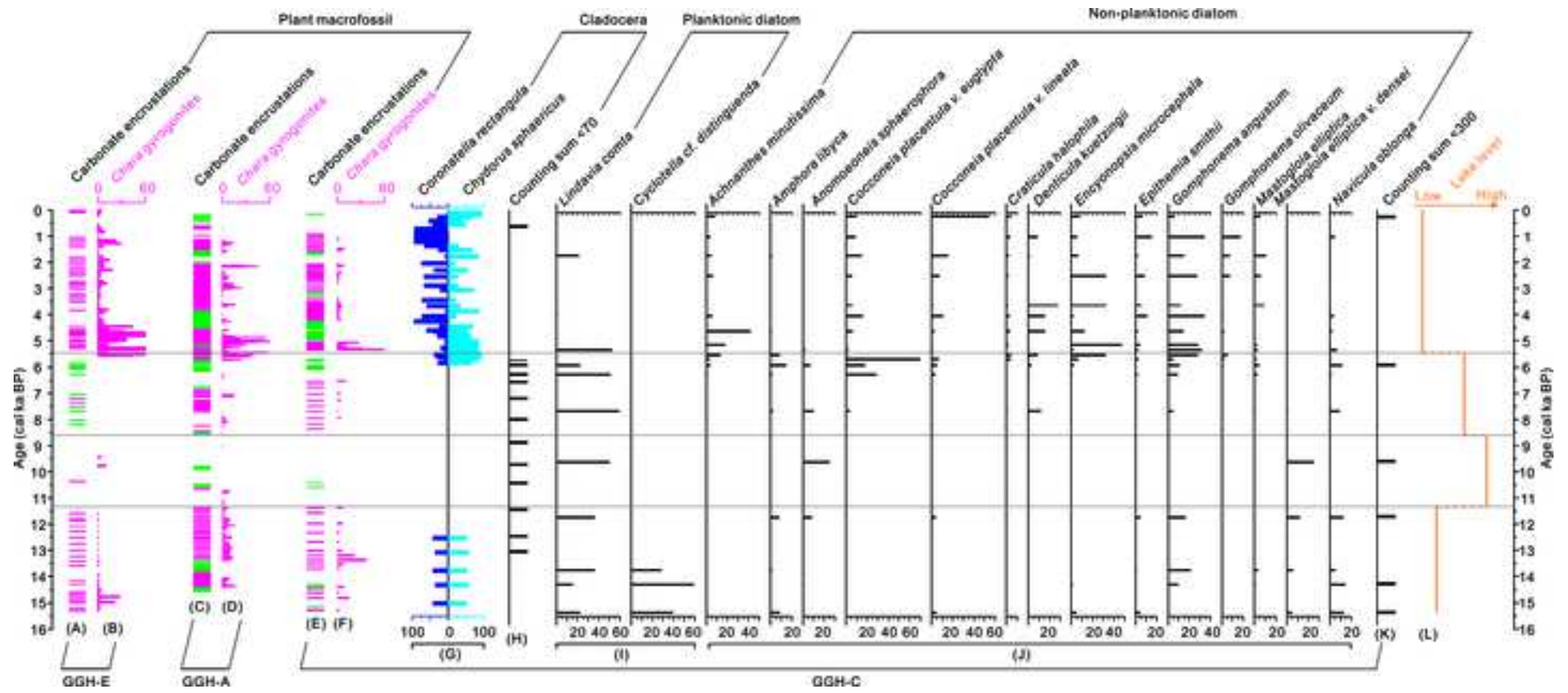


Fig. 2



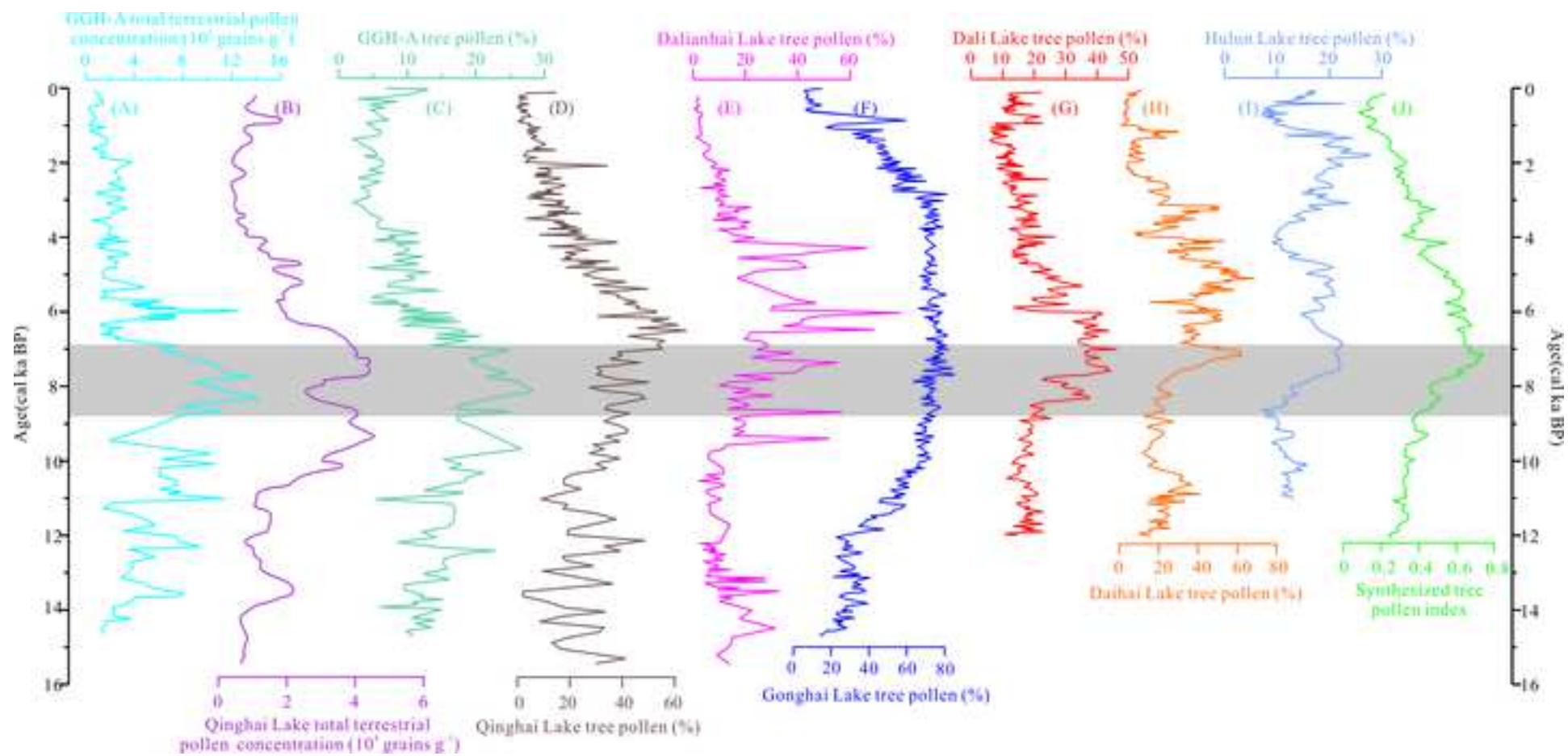
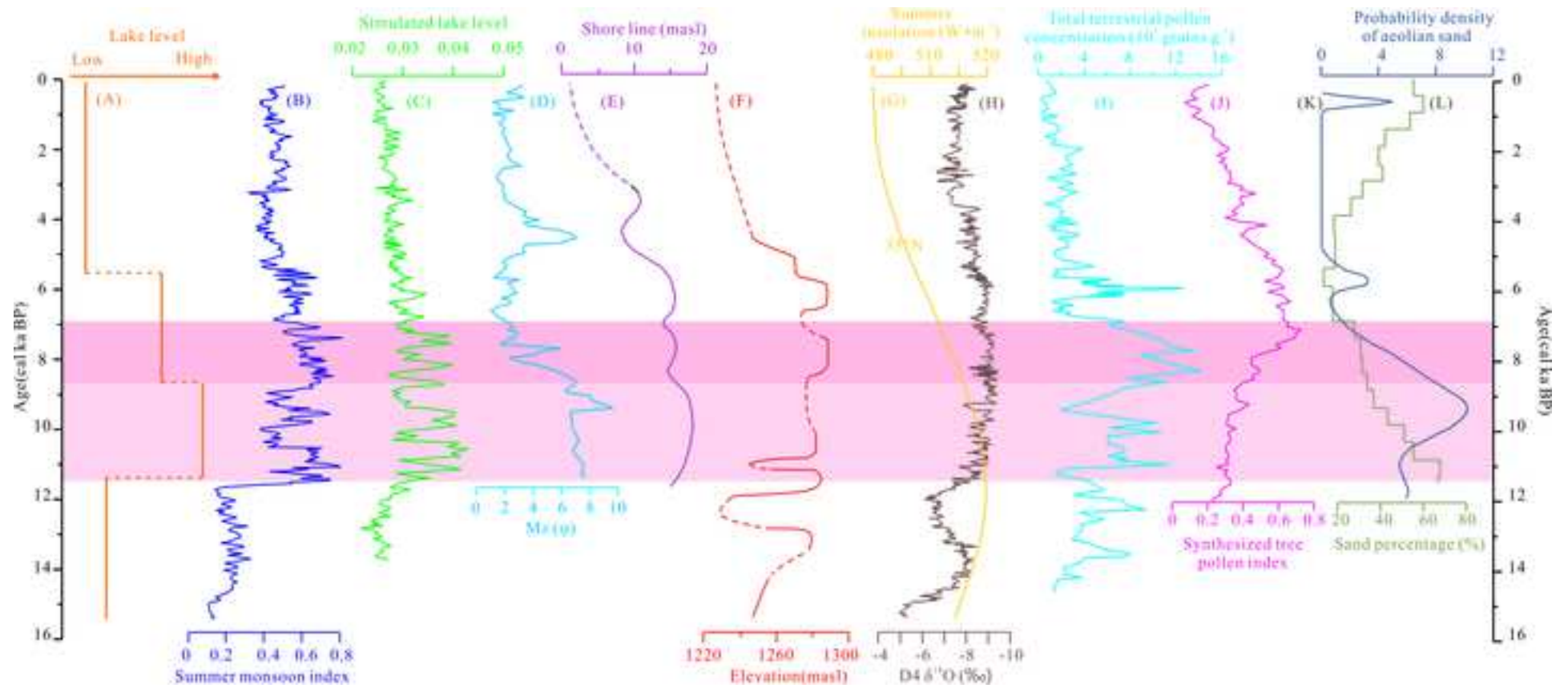
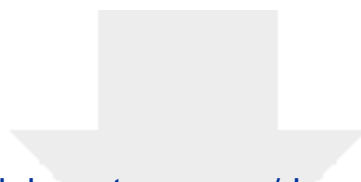


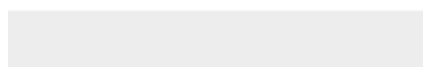
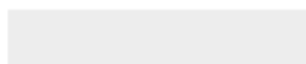
Fig. 4





[Click here to access/download](#)

Supplementary material for on-line publication only
Supporting Information V2.docx



Declaration of interests

The authors declare that they have no known competing financial interests or personal relationships that could have appeared to influence the work reported in this paper.

The authors declare the following financial interests/personal relationships which may be considered as potential competing interests: